# Protective effects of perennial ryegrass alleviating bone loss via gut microbiota through Wnt10b/NF-κB modulation in meat-type geese

Zeshan Zulfiqar[1†], Muhammad Arslan Asif[1†], Jiawen Cheng[1], Saira Saif[1], Nasir Mukhtar[2], Boshuai Liu[1,3,4], Yalei Cui[1,3,4], Yinghua Shi[1,3,4*]

[1]Department of Animal Nutrition and Feed Science, College of Animal Science, Henan Agricultural University, Zhengzhou, China

[2]Department of Poultry Science, Arid Agriculture University Rawalpindi, Pakistan

[3]Henan Key Laboratory of Innovation and Utilization of Grassland Resources, Zhengzhou, China

[4]Henan Forage Engineering Technology Research Center, Zhengzhou, Henan, 450002, China

[†]These authors contributed equally to this work.

[*]Correspondence: Yinghua Shi **(**annysyh@henau.edu.cn**)**

## ABSTRACT

### Background

Bone disorders in poultry are characterized by leg abnormalities, and alterations in the gut microbiota have been linked to the destruction of bone structure, which increases the risk of fractures. Ryegrass has antimicrobial, antioxidant and anti-inflammatory properties to improve the bone heath by regulating the gut microbiota.

### Purpose

In this study, we investigated the anti-inflammatory potential of perennial ryegrass to modulate the inflammatory bone loss in meat geese through regulating gut microbiota.

### Study design

The meat type geese were used to evaluate the efficacy of perennial ryegrass on bone health through core pathways.

### Methods

High-through 16sRNA (variable region V3-V4) sequencing was performed to determine the effect of Ryegrass intake on the gut microbiome of the meat geese. Biochemical indicators, Micro-CT, histopathology, immunofluorescence, western blotting were used to reveal the therapeutic potential of ryegrass to improve the bone health.

### Results

Ryegrass intake significantly reduced the inflammatory response (IL-1β, IL-18 and TNF- α) by improving the gut barrier function. Ryegrass improved Tibia BMD, ash% and tibia bone mineral contents. Results of gut microbiota and micro-CT analysis showed that the beneficial effect of Ryegrass on bone mass might be associated with higher relative abundance of short-chain fatty acids (SCFAs) producing gut microbiota in the cecum by improving microbial diversity. Ryegrass reduced the cecal mRNA expression of E.coli (a potent activator of LPS). Regarding bone turnover, Ryegrass increased the Wnt10b and other bone markers (ALP, RUNX2, OPG, OCN, SMAD) expression by reducing the NF-κB expression and bone resorption markers (NFATC1 and TRAF-6). It also decreased osteoclast number and (TRAP) activity. Ryegrass grazing exhibited an increase in the antioxidant capacity by increasing CAT and GSH-PX resulting in reduced ROS and MDA production. Western blot and Immunofluorescence analysis of tibia showed higher expression of Wnt-10b and reduced expression of NF-κB in GD group as compared to CD.

### Conclusion

These results indicates the importance of Perennial Ryegrass in alleviating bone through gut microbiota via different mechanism. These findings highlight the importance of gut-bone axis and provide new insight regarding the role of ryegrass on bone health in meat geese.


**Keywords**: Gut microbiota, SCFA, Bone, Inflammation, Geese

**Abbreviations:** ALP, Alkaline phosphatase; BCL-1, Beclin-1; BMD, Bone mineral density; BMP, Bone morphogenetic protein; BS, Bone surface; BUN, Blood urea nitrogen; BV, Bone volume; CaBP-28, Ca

binding protein; FGF-23, Fibroblast growth factor-23; GLU, Glucose; GPR, G-coupled Protein Receptor; HDAC, Histone deacetylase; HDL, High density lipoprotein; HIF, Hypoxia inducible factor; IGF-1, Insulin like Growth Factor-1; IL, Interleukin; LDL, Low density lipoprotein; LPS, Lipopolysaccharide; MEPE, Matrix extracellular phosphoglycoprotein; MyD88, Myeloid differentiation primary response 88; NF-κB, Nuclear Factor kappa-light-chain-enhancer of activated B cells; NrF2, Nuclear factor erythroid 2–related factor 2; OC, Osteoclast; OCN, Osteocalcin; OB, Osteoblast; OPG, Osteoprotegerin; PHEX, Phosphate regulating Endopeptidases X-linked; PMCA1b, Plasma membrane Ca+2 ATPase; PTH, Parathyroid hormone; RANKL, Receptor activator of nuclear factor kappa beta ligand; ROS, Reactive oxygen species; Runx2, Runt-related transcription factor2; SCFA, Short chain fatty acids; SMAD, Suppressor of mother against decapentaplegic; Tb.N, Trabecular number; Tb.Th, Trabecular Thickness; TD, Tibial Dyschondroplasia; Th, T-helper; TGF, Transforming growth factor; TJP, Tight junction proteins; TLR-4, Toll like receptor; TNF, Tumor necrosis factor; Tregs, T-regulatory; TRAF-6, Tumor necrosis factor receptor associated factor 6; TRAP, Tartrate resistant acid phosphatase; TS, Tissue surface; TV, Trabecular volume; VEGFA, Vascular endothelial growth factor; Wnt, Wingless-related integration site; μCT, Micro-computed tomography

## INTRODUCTION

The intensification of poultry farming worldwide increases stress and inflammation, posing significant challenges to bird health and productivity (Korver, 2023). Consequently, the poultry industry is increasingly confronted with various stressors, including environmental factors, nutritional deficiencies, and pathogen exposure. These challenges can lead to immune dysfunction (Li et al., 2015). Specifically, immune dysfunction manifests as chronic inflammation, adversely affecting poultry growth, reproduction, and overall health (Oke et al., 2024). Immune stress compromises the intestinal barrier and leads to digestive disorders, triggering inflammatory diseases, reduced production performance, and even mortality (Zhang et al., 2020). The inflammatory response can also disrupt normal physiological processes, leading to conditions such as skeletal disorders, a growing concern in poultry management, particularly in geese (Song et al., 2021). As a result, skeletal issues like valgus/varus deformities, tibial dyschondroplasia (TD), bone torsion, and fractures have become increasingly common in domestic birds with a prevalence rate of 20-30% (Hartmann and Flock, 1979).

Moreover, bone disorders, including leg abnormalities, pose both welfare and production concerns. For instance, 14–21% prevalence rates in commercial meat ducks have been associated with impaired mobility, pain, and difficulty accessing food and water, ultimately compromising growth performance (Jones and Dawkins, 2010; Xu et al., 2022). These disorders result from a complex interplay of pathological, nutritional, and environmental factors (Rath et al., 2000; Wang et al., 2022). Research indicates that these disorders may be exacerbated by inflammatory processes that alter bone metabolism, highlighting the need for a deeper understanding of the underlying mechanisms (Wang et al., 2022). The relationship between inflammation and bone health is complex, and addressing these challenges in poultry farming requires a comprehensive approach.

In this context, the gut microbiota plays a crucial role in maintaining bone health by influencing digestive processes, systemic inflammation and bone metabolism. Notably, dysbiosis in the gut microbiome has been observed in osteoporosis patients and rodent models subjected to ovariectomy (Seely et al., 2021), highlighting its impact on bone integrity. Modulating the gut microbiota—whether through germ-free environments, antibiotics, or probiotics—significantly affects bone quality and remodeling by influencing the interactions between the immune, endocrine, and calcium absorption (D'Amelio and Sassi, 2018). A critical factor in this process is the production of short-chain fatty acids (SCFAs) through gut microbiota fermentation, which benefits bone health by reducing inflammation and enhancing mineral absorption (Smith et al., 2013). Consequently, this connection between gut health and skeletal integrity highlights the need to explore further gut-bone interactions, particularly in poultry farming, to mitigate bone disorders through dietary interventions.

Naturally occurring inflammatory conditions in poultry often arise from bacterial infections, making LPS a useful model to study the impact of chronic inflammation on bone formation. When LPS activates Toll-like receptor 4 (TLR4), it triggers an immune response that releases pro-inflammatory cytokines, leading to inflammatory osteolysis (Lorenzo et al., 2008). This activation also engages the nuclear factor kappa B (NF-κB) signaling pathway, which plays a significant role in regulating cytokine expression. Additionally, NF-κB promotes osteoclastogenesis by upregulating key differentiation genes and prolonging osteoclast survival (Yamashita et al., 2007). Conversely, Wnt10b, a member of the Wnt signaling pathway, is critical for bone formation and has been shown to inhibit NF-κB activity through various molecular interactions (Die et al., 2012). Activation of the Wnt/β-catenin pathway stabilizes β-

catenin, which then suppresses NF-κB signaling in the nucleus (Liu et al., 2022; Ma and Hottiger, 2016). This interaction enhances osteoblastogenesis, inhibiting mesenchymal stem cells (MSCs) differentiation into adipocytes, ultimately promoting bone mass and strength (Cawthorn et al., 2012). Thus, the intricate balance between Wnt10b and NF-κB pathways is central to maintaining animal bone homeostasis.

Short-chain fatty acids (SCFAs), metabolic byproducts of gut microbiota, have also been implicated in bone health. SCFAs such as butyrate have been shown to inhibit histone deacetylase (HDAC) and modulate osteoclast gene expression, thereby promoting bone homeostasis (Karakan et al., 2021; Whisner et al., 2016). Additionally, SCFAs facilitate calcium absorption by lowering intestinal pH, enhancing mineral availability for bone formation (Whisner et al., 2016). Butyrate promotes the expression of osteoblast-related genes, such as RUNX2 and bone morphogenic protein-2 (BMP-2). Then, it influences bone formation via the BMP/SMADs and Wnt signaling pathways (Zhong et al., 2021). This highlights the potential for dietary interventions that can modulate gut microbiota and SCFA production to support skeletal health in poultry.

Geese are herbivorous and possess a unique ability to utilize high-fiber feeds, making them well-suited for efficiently digesting ryegrass (Yin and Huang, 2016). In China, ryegrass is the most commonly available pasture. It is rich in essential nutrients, including protein, dietary fiber, fatty acids, iron, zinc, magnesium, calcium, vitamins, essential amino acids, alkaloids, steroids, flavonoids, glycosides, phenols, and tannins (Chilibroste et al., 2000). Recent studies indicate that ryegrass can regulate intestinal microflora in geese (Zheng et al., 2021) and improve various ethno medical properties, such as antioxidant, antimicrobial, and anti-inflammatory effects in animals (Choi et al., 2017).

One of the critical interventions for enhancing poultry health is incorporating ryegrass into their diets. Its prebiotic properties can improve gut microbiota composition and increase short-chain fatty acid (SCFA) production (Tyagi et al., 2018; Zhang et al., 2021). By promoting a healthy gut environment, ryegrass is essential in modulating inflammatory responses, a key factor in maintaining poultry health (Ali et al., 2022). In this study, we aimed to investigate the role of perennial ryegrass (a fiber-rich, naturally available forage—as a novel dietary intervention) in alleviating bone loss in meat-type geese through modulating gut microbiota via Wnt10b/ NF-κB signaling mechanism. We evaluated changes in gut microbiota composition, SCFA levels, tibia bone structure, systemic inflammatory markers, and key signaling pathways such as Wnt10b and NF-κB. This comprehensive approach explored how Perennial Ryegrass may mitigate inflammatory bone loss and promote skeletal health in geese.

## MATERIAL AND METHODS

### Animals and Experimental Design

All experimental procedures were approved by the Institutional Animal Care and Use Committee of the Chinese Academy of Agricultural Sciences. Efforts were made to minimize animal suffering in accordance with the recommendations of the European Commission (Howe, 1997). All methods were conducted following the established guidelines. A total of 300 one-day-old Wanpu mixed-sexed geese bought from Henan Daidai Goose Agriculture and Animal Husbandry Development Co., Ltd (Zhumadian, China) having an average of 90 g (± 5.00), were split into two equal categories: (1) the commercially feeding group (CD, n = 150) and (2) the perennial ryegrass feeding group (GD, n = 150) with six replicates of 25 geese each. CD group fed a commercial diet according to company's recommendation (Supplementary table 1). GD group was given commercial feeding once a day (19:00h) in addition to 12 hours of ryegrass grazing (06:00-18:00h). The GD strategy was created by allowing meat geese to graze on ryegrass instead of other plants. Chick weight and feed intake were monitored at 15, 30, and 60 days of age to determine average daily gain (ADG), average daily feed intake (ADFI), and feed conversion ratio (FCR). Three diets were used in the experiment, Starter diet (1-20d), Grower diet (21-40d) and finisher diet (41-60d). Rye-grass nutritional profile was given in supplementary table 2. The trial was conducted for a period of sixty days.

### Sample Collections and Preparations

At 15, 30, and 60 days of age, three geese per replicate after a 12-h fasting period were slaughtered and blood samples were taken for serum analysis. Tissues and cecal chyme were separated and stored in liquid nitrogen at -80°C for further experimental analysis.

### Markers of oxidative stress and antioxidant defense

To assess the levels of LPS and ROS, CAT, GSH-PX and MDA, samples from serum, cecal tissues, and Tibia bone were taken. Shanghai Enzyme Link Biotechnology Co., Ltd. (Shanghai, China) supplied the kits, and all experimental methods were carried out in compliance with the guidelines provided by the manufacturer.

### Measurement of tight junction proteins

Tight junction proteins (Claudin and ZO-1) from the cecal tissues and serum DAO were quantified in compliance with the guidelines provided by the manufacturer (Shangai Mlbio Biotechnology Co., Ltd).

### Determination of inflammatory and anti-inflammatory factors

Serum, ceca and tibia samples were taken into sterile, enzyme-free centrifuge tubes and then IL-1B, IL-18, TNF-α and IL-10 from these 3 tissues were buy ELISA using a commercial Kit (Jiangsu Meimian Industrial Co., Ltd.) according to the manufacturer guidelines. Each assay included three tests on each of the samples.

### Morphological Analysis of Ileal and Cecal Tissue

Hematoxylin and eosin staining **(**H&E) staining was performed according the method used by (Ali et al., 2022a) to analyze the ileum morphology. Periodic acid-schiff (PAS) Staining of ceca were examined using an optimum microscope (40X magnification). Goblet cells were picked based on each visual field, and their numbers were identified with Image-J 6.0 Software (MD, USA).

**Determination of Lipid metabolism and bone hormonal profile**

Using a kit from Nanjing Jiancheng Bioengineering (Nanjing, Jiangsu, P. R. China), the following parameters were measured enzymatically: serum total cholesterol (T-CHO, #A111-1-1), low-density lipoprotein cholesterol (LDL-C, #A113-1-1), high-density lipoprotein cholesterol (HDL-C, #A112-1-1), triglycerides (TG, #A110-1-1), blood urea nitrogen (BUN, #C013-1-1), and glucose (GLU #B101-1-2). Bone modulating hormones, Estrogen, PTH, $1,25(OH)_2D_3$, ALP, serotonin and IGF-1 from the serum were quantified using an ELISA kit designed specifically for geese, as per the manufacturer's protocol (Nanjing Jiancheng Bioengineering Institute, Nanjing, China).

**Measurement of Tibia Parameters**

Tibia weight (g), length (mm), and breadth (mm), were measured with an electronic balance and digital Vernier caliper. According to (Riesenfeld, 1972), the robustcity index was determined as follows: robustcity index = bone length/cube root of the bone weight. The measurement of tibial dyschondroplasia (TD) lesion was done according to the method used by (Zhang et al., 2018). A mobile, fully automatic veterinary biochemistry analyzer (#SMT-120 V; Seamaty Technology Co., Ltd., Chengdu, China) was used to measure serum Ca and P. Tibia Ca, P and ash content were determined according to the method of (David et al., 2022). ELISA kit (Nanjing Jiancheng Biotechnology Co. Ltd, Nanjing, China) was used to quantify the bone markers OCN, TRAP, NFATC1, and TRAF6 from the tibia as directed by the manufacturer.

**Micro-CT tibia analysis**

After removing soft tissue, the tibia was dried at 65 °C to preserve its microstructure and prevent the water content of the bone from interfering. Initial testing revealed that the imaging process was unaffected by the procedure. Next, the tibia was photographed using the Bruker Skyscan 1176, a specially-made micro-CT scanner. Approximately 2000 projection images, comprising the whole 360° angular range, were obtained for every micro-CT scan, with each projection being exposed for 900 ms. At 11 W desired power, a 120 kV tube voltage was used. An additional 0.5 mm Al filter was employed to lessen the impact of beam hardening. The size of the reconstructed isotropic voxel, using geometrical magnification, was 223 µm3. Reconstructed projection data and micro-CT images were analyzed with customized scripts in Image J (National Institutes of Health, USA). The interesting trabecular and cortical bone (a 4 mm-long section) in the proximal part of the tibia was chosen 9 mm below the condyle surface. The bone volume to total volume ratio (BV/TV) and the trabecular thickness were calculated, and the overall volume and the volume of the trabecular bone were measured. The data obtained by r is reconstructed. CT vol software was used to reconstruct the images of the area of interest. The tibia bone mineral density (BMD) was measured using Dual-Energy X-Ray Absorptiometry (DEXA, Tokyo, Japan).

**Bone Histological Analysis**

Goldner trichome staining was performed according the protocol described by (Dobrowolski et al., 2017). This staining was employed to evaluate the morphology of the osteoid to mineralized bone ratio, mineralization. Tartrate-resistant acid phosphatase staining (TRAP) was performed according to the method elaborated by (Zhang et al., 2022) to measure the osteoclast number. Safranin O staining was performed according the protocol described by (Dobrowolski et al., 2017) to measure the proteoglycan content and articular cartilage thickness of different zones.

**Immunofluorescence (IF) analysis of Wnt10b and NF-κB**

Tissue slices of the tibia bone were soaked in 4% paraformaldehyde for ten minutes. The sections of paraffin were dewaxed with xylene for 15 minutes, then dehydrated with gradient alcohol and washed with distilled water. Cecal tissue section slides were dewaxed and rehydrated, then boiled in a citrate-EDTA antigen retrieval solution for 2 minutes before being blocked with 10% fetal bovine serum for 30. The tissue sections were incubated for Wnt10b and NF-κB with primary antibodies Rabbit Anti-Wnt10b (67201-1-IG, 1:500/1:200 v/v) and Rabbit Anti- NF-κB (CY2339, 1:500/1:200 v/v) at 4°C overnight, then treated with secondary antibody (HRP Goat Anti-Rabbit IgG (SeraCare, 5220-0336, 1:400; v/v) with incubation at room temperature in a dark place for 50 minutes. Tyramine sodium fluorescein was applied dropwise to the tissues (prepared with phosphate-buffered saline with Tween 20 (PBST) having 0.0003% H2O2) and incubated at room temperature for 20 minutes. The slides were incubated for 10 minutes at room temperature with 4',6-diamidino-2-phenylindole (DAPI). Following that, the slides were sealed with anti-fluorescent quenching mounting media, and the localization of Wnt10b and NF-κB was determined using a confocal fluorescence microscope (TCSSP8STED, Leica, Wetzlar, Germany). Under UV illumination, DAPI-stained nuclei appear blue and are positively shown as fluorescein-labeled green light.

**SCFA Analysis**

SCFA concentrations were determined by the method described by (Zhang et al., 2022).

**Gene expression assays**

Total RNA from the tibia bone and cecal tissues (50 to 100 mg) was extracted by adding 1 mL of MagZol-reagent (#R4801- 02; Magen Biotechnology, Guangzhou, Guangdong, China) per the manufacturer's instructions. The concentration and purity of total RNA were determined with a NanoDrop 2000 UV-vis spectrophotometer (Thermo Scientific, Wilmington, USA). The RNA was then reverse transcribed to cDNA through the ReverTra Ace® qPCR RT Master Mix with gDNA Remover (TOYOBO, OSAKA, Japan), following the manufacturer's instructions. The cDNA samples were amplified using a real-time quantitative polymerase chain reaction with Vazyme Biotechnology's ChamQ Universal SYBR qPCR Master Mix. Primer3web, version 4.1.0, was used to build gene-specific primers for all genes (Supplementary Table 3). PCR was carried out using the C1000 Touch PCR Thermal cycler (BIO-RAD Laboratories, Shanghai, China) with ChamQ Universal SYBR qPCR Master Mix from Vazyme Biotechnology (Nanjing, Jiangsu, P. R. China) as follows: 40 cycles of 15 seconds at 95°C followed by 30 seconds at 60°C. Each measurement was taken in triplicate. The 2-DDCT approach (Livak and Schmittgen, 2001) was used to calculate target genes messenger ribonucleic acid (mRNA) expression compared to GAPDH.

**Western Blot Analysis**

Tibia and duodenal protein were separated from liquid nitrogen snap frozen tibia by pulverizing the bone with a mortar and pestle and shifting the resulting powder (40 mg) to 0.4 mL of ice-cold radio immunoprecipitation assay (RIPA) lysis buffer (catalogue no. P0013B, Beyotime Institute of Biotechnology) enriched with 4 µL of protease inhibitor (catalogue no. B14001; BioTool). The lysates were sonicated for 10 seconds and 8 times in an ice-cold water bath before centrifugation to separate the protein extract. The resulting liquid was taken out for total protein determination via a bicinchoninic acid protein assay kit (catalogue no. 23225; Pierce). The extracted protein (30 µg) was electrophoresed on a 10% SDS-PAGE gel and electrotransferred onto polyvinylidene fluoride membranes (catalogue no. IVPH00010; Merck Millipore). Following the transfer, membranes were blocked for 1 hour at room temperature in a blocking solution containing 5% skimmed milk and then incubated overnight at 4 °C with the subsequent primary antibodies: Wnt10b (cat: A6124; Abclonal), RUNX2 (cat: A7918; Abclonal), OCN (cat: ab108073;

abcam), SMAD (cat: ab103203; abcam), ALP ( Cat: 27260-1-AP; Proteintech Biotechnology, Chicago, IL, USA), RANKL (Cat: 60291-1-Ig; Proteintech Biotechnology), NFATC1 (Cat: ER1906-37; HUABIO, Hangzhou, China), PMCA1b (Cat: 14085; ABclonal), CaBP-28K (Cat: 511369; ZenBio, Chengdu, China), VEGFA (Cat: 350146; ZenBio), HIF (Cat: 340629; ZenBio), NF-κB p65 (Cat: ET1603-12; HUABIO), NPt2a (Cat: ET1604- 27; HUABIO), PHEX (cat: HX1827; Huaxingbio), FGF-23(Cat: AC032; ABclonal, Wuhan, China), HDAC (Cat: 35098; ABclonal, Beijing, China), OPG (Cat: AR05; ABclonal, Wuhan, China)and β-actin (Cat: AC026; ABclonal, Wuhan, China). The blots were visualized utilizing a Western blotting detection system, and the protein concentrations in each sample were normalized to the abundance of β-actin.

**Analysis of 16S rRNA Gene Sequencing**

**DNA extraction and PCR amplification:**

Total microbial genomic DNA was isolated from cecal chyme samples via the E.Z.N.A.® soil DNA Kit (Omega Bio-tek, Norcross, GA, USA) according to the manufacturer's instructions. The DNA quality and concentration were evaluated using 1.0% agarose gel electrophoresis and a NanoDrop2000 spectrophotometer (Thermo Scientific, United States) and stored at -80 ℃ for future use. The hypervariable region V3-V4 of the bacterial 16S rRNA gene was amplified using primer pairs 338F (5'-ACTCCTACGGGAGGCAGCAG-3') and 806R (5'-GGACTACHVGGGTWTCTAAT-3') in a T100 Thermal Cycler PCR thermocycler (BIO-RAD, USA). To create a 20 μL PCR reaction, add 4 μL of 5 × Fast Pfu buffer, 2 μL of 2.5 mM dNTPs, 0.8 μL of each primer (5 μM), 0.4 μL of Fast Pfu polymerase, 10 ng of template DNA, and ddH2O. The PCR amplification cycling conditions were the following: initial denaturation at 95 ℃ for 3 min, following 27 cycles of denaturing at 95 ℃ for 30 s, annealing at 55 ℃ for 30 s, extension at 72 ℃ for 45 s, and single extension at 72 ℃ for 10 min, and finish at 4 ℃. The PCR product was extracted from a 2% agarose gel, purified with the PCR Clean-Up Kit (YuHua, Shanghai, China) per the manufacturer's instructions, and quantified with Qubit 4.0 (Thermo Fisher Scientific, USA).

**Illumina PE300/PE250 sequencing**:

Purified amplicons were pooled in equimolar levels and paired-end sequenced on an Illumina PE300/PE250 platform (Illumina, San Diego, USA) using standard techniques by Majorbio Bio-Pharm Technology Co. Ltd. (Shanghai, China). The raw sequencing reads were uploaded to the NCBI Sequence Read Archive (SRA) database (Accession Number: PRJNA1158539).

**Amplicon sequence processing and analysis:**

Following demultiplexing, the sequences were quality-filtered with fastp (0.19.6) and combined with FLASH (v1.2.11). The high-quality sequences were de-noised using the DADA2 Deblur plugin in the Qiime2 (version 2020.2) pipeline with suggested values, resulting in single nucleotide resolution based on error patterns within samples. Deblur-denoised DADA2 sequences are commonly referred to as amplicon sequence variations (ASVs). To reduce the impacts of the depth of sequencing on alpha and beta diversity measurements, the number of sequences from all samples was limited to 20,000, resulting in an average Good's coverage of 97.90%. ASV taxonomy was assigned using Qiime2's Naive Bayes (Vsearch, Blast) consensus taxonomy classifier with the SILVA 16S rRNA database (v138).

Bioinformatic analysis of the gut microbiota was performed on the Majorbio Cloud platform (https://cloud.majorbio.com). Mothur v1.30.1 was used to produce alpha diversity indices, which included observed ASVs, Simpson, Sob and Ace. Principal coordinate analysis (PCoA) based upon Bray-Curtis dissimilarity was used to determine the similarity of microbial communities across various samples using

the Vegan v2.5-3 software. Circos diagram was used to demonstrate the microbial abundance at genus level. The linear discriminant analysis (LDA) effect size (LEfSe) (http://huttenhower.sph.harvard.edu/LEfSe) identified the significantly numerous taxa (phylum to genera) of bacteria among the different groups (LDA score > 2, $P < 0.05$). A correlation among two nodes was regarded as statistically significant if Spearman's correlation coefficient was greater as 0.6 or less than -0.6, with a P-value less than 0.01. To further investigate the impact of microbiota on apparent performance, redundancy analysis (RDA) at the genus level was carried out using the R language vegan package on Spearman correlation analysis (RDA 2014).

**Statistical Analysis**

Statistical analysis were performed using SPSS 20.0 software (=D3 SPSS, Inc., 2009, Chicago, IL, USA www.spss.com). All values were expressed as mean ± standard deviation. Two-tailed unpaired T-test was used to determine the statistical significance. Level of significance was considered to be at < 0.05 and $P < 0.01$.

## RESULTS

### Growth Performance

Indeed, Wanpu-geese (GD) had a lower feed intake, ADG and F:G ratio than the commercial feeding group (CD) mainly due to the higher locomotor activity, with a lower solid feed consumption due to the pasture intake (Figure 1a-c). The estimation of forage intake in birds reared free range is difficult and only few studies have been carried out mainly with laying hens.

### Tibia characteristics and their growth plates

To determine the changes in tibia related parameters in geese in the CD and GD groups, relative tibia weight, Length and width were measured at 15th, 30$^{th}$ and 60$^{th}$ day. Ryegrass intake had no effect on relative tibia weight at day 30 ($P<0.05$) significantly (Figure 1d). Tibia width remained unaffected (Figure 1f). Ryegrass feeding increased the Robustcity index significantly at Day 30 ($P<0.05$) (Figure 1g). CD group had higher growth plate width leadings towards increased TD lesion as compared to GD group (Figure 1h, s).

### Serum and Tibia indices

Serum Ca content remained unaffected ($P>0.05$) in both CD and GD groups (Figure 1i), where there was significant increase ($P>0.05$) in Tibia Ca on Day 15, 30 and 60 (Figure 1j). Ryegrass feeding resulted in a significant increase ($P<0.05$) in serum and Tibia phosphorus content (Figure 1k-l). Ryegrass feeding increased ($P<0.05$) the bone formation marker known as ALP (Alkaline Phosphatase) significantly (Figure 1m-n) and decreased ($P<0.05$) the bone resorption marker TRAP (Figure 1o) significantly in serum. Tibia OCN also known as (BGLAP) was significantly increased ($P>0.05$) in GD group (Figure 1p). There was a significant reduction ($P<0.05$) in bone resorption agents known as NFATC1 and TRAF6 in GD groups as compared to CD group on Day 15, 30 and 60 (Figure 1q-r).

### Trabecular and cortical microstructure of tibia

Ryegrass feeding was very effective in increasing the BS/TV%, Tb.N, Tb.Th significantly at Day 15, 30 and 60 ($P<0.05$) of Trabecular bone. There was also a significant increase in BMD on Day 30 and 60 ($P<0.05$) in GD group and as compared to CD group in trabecular section. BV/TV% and TS increased significantly on Day 15 and 60 ($P<0.05$) as a result of ryegrass feeding. Trabecular BS/BV% was higher ($P<0.05$) in GD group on Day 30 and 60 as compared to CD group. Ryegrass intake lowers the Tb.sp significantly ($P<0.05$) in GD on Day 15, 30 and 60. (Figure 2a). Regarding Cortical bone, there was significant improvement ($P<0.05$) in BV/TV, TS, BS/BV and BS/TV on Day 15, 30 and 60 in GD group as a result of ryegrass feeding. BMD of cortical bone was increased significantly ($P<0.05$) in GD group on Day 30 and 60 (Figure 2b).

### Histological analysis of Tibia Bone

Three staining techniques were performed to evaluate the changes in tibia bone due to LPS production. Goldner trichome staining was used to evaluate the osteoid and mineralized area of the tibia bone. Green color represented mineralized bone and red color represented the osteoid portion. Collagen area of the tibia were significantly higher in CD group (Figure 2c). Ryegrass intake reduced the osteoid-to-mineralized ratio and increased the mineralized portion as compared to CD (Figure 2c). TRAP staining was performed to measure the osteoclast area and number. Tibia TRAP activity and Osteoclast number was

significantly reduced in GD group (P<0.01) as result of ryegrass intake (Figure 2d). Safranin O staining was to check the articular cartilage pattern and proteoglycan content. There are no irregularity in the pattern of cartilage on both groups. On day 15, zone II and total thickness of articular cartilage were significantly increased (P<0.05) in GD group. On day 30, zone I, II, III and total thickness were higher as a result of ryegrass grazing. Zone I and total thickness of articular cartilage were higher (P<0.05) on day 60 in GD group. Dark Red color represented higher proteoglycan and less intensity of red color represented less proteoglycan content. Ryegrass intake significantly increased the proteoglycan content in GD group in comparison with CD group (Figure 2e).

**Ryegrass intake improves the antioxidant status in serum, tibia and ceca**

To check the antioxidant capacity of Ryegrass feeding, protein levels of antioxidants GSH-PX and CAT from serum, tibia and ceca samples of meat geese at 15d, 30d, and 60d were measured. There was significant increased (P<0.01) in GSH-PX in the serum day 15 and 30, in the tibia on day 15 (P<0.05), 30 (P<0.05), and 60 (P<0.05) and in the ceca on day 15, 30 and 60 (Figure 3a-c). CAT was also significantly increased (P<0.05) in serum on day 15, 30 and 60, in the tibia and ceca on day 15 and 60 (Figure 3d-f). Further, whether these antioxidants are involved in attenuating the mediators that caused ROS insults in CD and GD meat geese, we measured oxidative mediator MDA from serum, tibia and cecal samples. We examined a severe increase in the levels of MDA in CD meat geese compared with GD meat geese at three time points 15d, 30d, and 60d (Figure 3g-i).

**Ryegrass intake improved the metabolic profile in meat geese**

The Ryegrass grazing system was effective in preventing metabolic syndrome in GD meat geese with a significant improvement in body metabolic profile. HDL was significantly increased (P<0.01) in GD group on day15, 30 and 60 (Figure 3m). Triglycerides, Cholesterol, LDL, and GLU were significantly (P<0.01) higher in CD group as compared to GD group on day 15, 30 and 60 (Figure 3k-l, o). Blood urea nitrogen was significantly higher (P<0.01) in CD group meat geese on day 15 and 30 as shown in the (Figure 3n).

**Ryegrass feeding regulated the bone modulating hormones**

To check whether Ryegrass intake regulated bone modulating hormones, ELISA was performed to check their levels in the hormones. There was a significant increase in Estrogen (P<0.05) on day 15, 30 and 60 (Figure 3p). Calcitonin was also significantly increased (P<0.05) on day 15, 30 and 60 (Figure 3t). Vitamin $D_3$ and IGF-1 were also significantly increased (P<0.05) on day 30 and 60 (Figure 3q,u). Compared with GD group, CD had significantly higher (P<0.05) level of serotonin (5-HT) on day 15, 30 and 60 (Figure 3r). PTH level was significantly higher (P<0.05) on day 15,30 and 60 in CD group as compared to GD group (Figure 3s).

**Intestinal Microflora of the Wanpu Meat geese**

**Structural composition at Phylum level**

High-through 16sRNA (variable region V3-V4) sequencing was performed to determine the effect of ryegrass intake on the gut microbiome of the meat geese. The metagenome predicted functions classified using clusters of orthologous genes (COG) database in phylogenetic reconstruction of unobserved states software are performed to investigate the functional differences in the gut microbiota between the two

feeding meat geese groups; commercial feeding group (CD) and Ryegrass feeding group (GD) meat geese) at different time points 15d, 30d, and 60d. To identify which strains, contribute to LPS production in the meat geese gut, we focused on the GO terms and cecal microbiota at the phylum level mainly relevant to LPS biosynthesis. At 15d, in the CD group, *Bacteroides* families dominated the four while *Actinobacteiota* dominated over *Verrucomicrobiota* related to LPS biosynthesis. At 30d, in the CD group, *Firmicutes* families dominated the four related to LPS biosynthesis, respectively. At 60d, only *Firmicutes* family dominated the four main COG terms related to LPS biosynthesis in CD group geese. Overall, *Firmicutes* and *Bacteroidota* families dominate both in the CD and GD meat geese at 15d, 30d, and 60d, but *Firmicutes* and *Bacteroidota* individually contribute 85.96% and 15.24% of the LPS biosynthesis in the CD meat geese at 30d and 60d, respectively (Figure 4a-c). In contrast, *Actinobacteriota* family is the minor contributor to LPS biosynthesis, with an average of 2.85% of the total LPS biosynthesis in CD meat geese at 15d. In contrast to other bacterial families, *Proteobacteria* family with a minute quantity with an average of 2.94% contributes to the total LPS biosynthesis in CD meat geese at 60d. Figure 4(a-c) represented the microbial diversity at phylum level.

**Microbial diversity in response to Ryegrass feeding**

The cecal microbial community in geese feeding ryegrass increased richness and evenness but the difference was no significance (P>0.05). There was no significant difference in alpha diversity (Simpson, Shannon and Ace index) on all three phases as shown in Figure 4(d-f). A significant difference in beta diversity ($P < 0.05$) was observed in the GD group on Day 15 (Figure 4g). However, no significant separation ($P > 0.05$) was detected between the two groups on Days 30 and 60 (Figure 4h-i).

**Structural Composition at Genus level**

The quality and types of diet make alterations in the gut microbiota in a time-dependent manner. Ryegrass intake modulated the gut microbial community at the genus level. We sorted out the 20 bacteria at the genus level related to bone health. The relative abundance of *Streptococcus, Ruminococcus, Oscillospiracae, Faecalbacterium, Lactobacillus, Butyricoccus, Bifidobacterium, Lachnospiracae, Gastranaerophilales, Allistipes, Bacteroides, Barnesiella, Akkermansia, Blautia* and *Rombutsia* were significantly higher (P<0.01) in GD group as a result of Ryegrass intake. Compared with GD group, CD group has significantly higher (P<0.01) relative abundance of *Erysipelatoclostridium, Rikenellaceae_RC_gut_group, CUCG14*, *Subdoligranum*, and *E.coli* (Supplementary Figure 1). We found the abundance of E.coli in CD group. E.coli is the potent activator of LPS and other inflammation causing agents. To confirm the abundance of E.coli, we performed qPCR to find the expression of it. It was shown from the mRNA expression that E.coli was significantly enhanced in commercial feeding group (CD) as compared to the GD group as shown in the Figure 7(s). Circos diagram represented the diversity and abundance of bacterial genera across CD and GD groups helping to visualize the microbiome composition and identify patterns or relationships among bacteria in response to treatment. This visualization aids in understanding how different treatments or time points impact the microbial community structure (Figure 4j-l).

**LPS production affected by Gut Microbiota**

Spearman's correlation analysis was performed to identify the relationship between Gut microbiota and LPS production. A total of 14 genera regarding bone health were common between CD and GD groups.

On Day 15, E.coli was positively correlated with LPS in the bone marrow and LPS synthesizing gene rfaL. Shigella was also positively correlated with rfaL. *Rikenellaceae_RC_gut_group* and *Subdoligranum* had a positive correlation with TLR-4. There was also a positive correlation between C-UCG-14 and LPS (bone marrow), TLR-4 and LPS synthesizing gene rfaK. Others genera *Ruminococcus, Faecalbacterium, Blautia and Akkermansia* were negatively correlated with LPS and its synthesizing genes as shown in the figure 5(a).

On Day 30, E.coli was positively correlated with LPS in the bone marrow. *Subdoligranum* was highly positively correlated with LPS (Ceca) and and its synthesizing genes (fraK and rfaL). *Rikenellaceae_RC_gut_group* had also a positive correlation with LPS production from serum and bone marrow, TLR-4 and LPS synthesizing genes (rfaK and rfaL). *Lactobacillus, Akkermansia, Alistipes* and other are negatively correlated with LPS and its sysnthesizing genes as shown in the figure 5 (b).

On day 60, *Rikenellaceae_RC_gut_group* had a positive correlation with LPS (Bone marrow), TLR-4 and rfaL. *Subdoligranum* showed the similar trend except LPS (ceca). *Shigella* and *C-UCG-14* were positively correlated with LPS (ceca), TLR-4 and rfaL. *Blautia, Bifidobacterium* and *Bacteriodes* was negatively correlated with LPS production as shown in the figure 5(c).

**LefSe Analysis**

LefSe analysis was performed to identify the specific bacteria being differentially expressed in CD and GD groups. On Day 15, compared with GD group, *E.coli* and *CUCG-014* showed an increased abundance in CD group. *Ruminococcus, Faecalbacterim* and *Bifidobacterium* were higher in GD (Figure 4j). On Day 30, *Enterococcus* and *E.coli* were highly abundant in CD groups while *Allistipes, Blautia* and others were highly abundant in GD group (Figure 4k). On day 60, *Enterococcus, Shigella, Subdoligranum*, and *Shuttle worthia* showed higher abundance in CD group and *Actinobacteria, Bifibacteriales* and *oscillospiracae* were higher in GD group as shown in the figure 4(l).

**Ryegrass intake increases the SCFA's Production**

Short chain fatty acids are the main metabolites generated by gut microbiota. In the present study, Ryegrass intake had a significant effect on SCFA's levels. Ryegrass supplementation through natural grazing system increased acetate production significantly ($P<0.05$) at Day 15, 30 and 60 (Figure 3v). Propionate and Butyrate levels were significantly increased as shown the Figure (Figure3 w-x). Ryegrass intake significantly increased ($P<0.01$) the levels of Iso-butyrate, isovaleric acid and valeric acid (Figure3 y-z, aa).

**Ryegrass intake improved intestinal morphology**

Compared with the commercial feeding group (CD), histological analysis showed that ryegrass intake increased villus height ($P<0.01$), width ($P<0.01$) villus surface area ($P<0.01$, $P<0.05$), V:C ratio ($P<0.01$) as shown in the figure 6 (a-b, d-e) and decreased crypt depth ($P<0.05$) of the ileum on day 15, 30 and 60 (Figure 6c). Regarding Cecal histology, mucosal and muscularis thickness were also significantly increased ($P<0.01$) as a result of ryegrass feeding on day 15, 30 and 60 (Figure 6 f-g). Periodic acid-schiff (PAS) Staining was performed to calculate the number of goblet cells. Goblet cells were significantly increased ($P<0.01$) in GD group as compared to CD group on day 15, 30 and 60 (Figure 6h). Histological pictures of ileum and ceca were shown in the supplementary Figure 6-**I**.

**Gut Permeability Indices**

To determine the gut permeability, Serum DAO was checked using ELISA. Ryegrass significantly lowered the DAO level (P=0.05, P<0.01) on day 15 and 30 (Figure **6-II**i). Furthermore, the expression of tight junction proteins was examined using immunohistochemical analysis. The results showed that ryegrass feeding significantly increased the level of ZO-1 (P<0.01) on day 15, 30 and 60 (Figure **6-II**j). Claudin-1 was also significantly increased (P<0.01) on day 30 and 60 (Figure **6-II**k). Immunofluorescence analysis (IF) of these tight junction proteins were shown in the Figure (**6-II**) respectively.

**Ryegrass intake modulated immune response by regulating intestinal barrier function**

Compared with CD group, Ryegrass intake lowered the level of proinflammatory cytokines. IL-1B was significantly reduced (P<0.01) in serum, tibia on day 15, 30, 60 and also in the ceca on day 30 and 60 in GD group (Figure 7 a-c). There was also significant reduction (P<0.05) in the levels of IL-18 and TNF-α (P<0.01) as a result of Ryegrass feeding (Figure 7 d-i). On day 15, GD group has significant increase (P<0.05) IL-10 levels in serum and tibia. There was a highly significant production (P<0.01) of IL-10 in serum, tibia and ceca on day and also significant higher (P<0.05) levels on day 60 (Figure 7 j-l). LPS production was significantly higher in commercial feeding groups. In serum, LPS production was highly significant (P<0.01) on day 30 and 60 in CD group. In tibia, LPS was higher (P<0.05) day 15 and significantly higher (P<0.01) on day 30 and 60 as a result of commercial feeding. Ceca has also higher levels (P<0.05) in CD group as compared to GD group on day 30 and 60 (Figure 7 m-o). GD group had significantly lower (P<0.01) levels of ROS production as a result of ryegrass feeding in tibia on day 15 and 30. In serum, ROS production was significantly reduced (P<0.01) in GD groups as compared to CD group. Cecal ROS was significantly higher (P<0.01) on day 15, 30 and also on day 60 (P<0.05) commercial feeding groups (CD) as compared to ryegrass grazing group (GD) as shown in the Figure 7 (p-r).

**Correlation between Gut Microbiota and SCFA's**

On day 15, Ruminococcus was highly positively correlated with acetic acid. *Faecalbacterium, Alistipes, and Bacteroides* showed highly positive correlation with propionic acid. *Blautia, Alistipes* and *Bacteroides* were highly positively correlated with butyric acid. *Faecalbacterium, Alistipes* and *Bacteroides* showed high positive correlation with iso-butyric acid. *Lachnospiraceae* and *Bifidobacterium* was positively correlated with iso-valeric acid. *Ruminococcus, Faecalbacterium, Lachnospiraceae* and *Bifidobacterium* had positive correlation with Valeric acid. *E.coli, Shigella, Rikenellaceae_RC_gut_group, C-UCG-14* and S*ubdoligranum* were negatively correlated with short chain fatty acids as shown in the figure 5 (d).

On day 30, *Ruminococcus* and *Bifidobacterium* were highly positively correlated with acetic acid and propionic acid. *Lactobacillus* was highly positively correlated with butyric acid. *Lachnospiraceae* showed extremely high positive correlation with iso-valeric acid. *Bacteroides* was positively correlated with *Valeric acid. E.coli, Rikenellaceae_RC_gut_group, C-UCG-14* and *Subdoligranum* were negatively correlated with short chain fatty acids as shown in the figure 5 (e).

On day 60, *Lachnospiraceae* was highly positively correlated with acetic acid. *Bacteroides* showed extremely high positive correlation with propionic acid. *Alistipes* and *Bifidobacterium* were highly positively correlated with butyric acid. *Lactobacillus* showed high positive correlation with iso-butyric acid and iso-valeric acid. *Ruminococcus, Blautia* and *Akkermansia* were positively correlated with Valeric acid.

*Rikenellaceae_RC_gut_group, C-UCG-14* and *Shigella* showed negative correlation with short chain fatty acids as shown in the figure 5 (f).

**Correlation between SCFA's, immunity and gut barrier function**

Spearman heatmap analysis was performed to elaborate how SCFA's improve immunity and gut barrier function leading to better bone health.

On Day 15, Acetic was negatively correlated with IL-1B (tibia), IL-18 (tibia) and TNF- α (serum) and positively correlated with ZO-1. Propionic acid was negatively correlated with IL-1B (tibia), IL-18 (ceca) and positively correlated with 1L-10 (serum and tibia) and Claudin-1. Butyric acid was negatively correlated with IL-18 (tibia and ceca) and positively correlated with IL-10 (serum, tibia and ceca) and Claudin-1. Iso-butyric was negatively correlated with IL-18 (ceca) and TNF- α (tibia) and positively correlated with IL-10 (serum and tibia) and Claudin-1. Iso-valeric acid was negatively correlated with IL-1B (serum), IL-18 (tibia), and TNF- α (tibia) and positively correlated with IL-10 (ceca). Valeric acid had a positive correlation with ZO-1 as shown in the figure 5 (g).

On Day 30, Acetic acid was negatively correlated with 1L-1B (serum, tibia and ceca), TNF- α (serum, ceca) and positively correlated with IL-10 (tibia). Propionic acid was negatively correlated with 1L-1B (serum, tibia and ceca), IL-18 (serum), TNF- α (ceca) and was positively correlated with IL-10 (serum). Butyric acid was negatively correlated with IL-1B (tibia), IL-18 (tibia) and TNF- α (serum) and positively correlated with Claudin-1. Iso-butyric acid was negatively correlated with IL-1B (tibia), TNF- α (serum, tibia) and positively correlated with IL-10 (tibia), ZO-1 and Claudin-1. Iso-valeric acid had negative correlation with IL-1B (serum), IL-18 (serum), TNF- α (serum, tibia) and positive correlation with IL-10 (serum). Valeric acid was negatively correlated with IL-18 (ceca), TNF- α (serum) and positively correlated with IL-10 (tibia) and Claudin-1 as shown in the figure 5 (h).

On day 60, Acetic acid and Butyric acid were negatively correlated with IL-18 (tibia), and positively correlated with IL-10 (tibia) and Claudin-1. Propionic acid followed the same trend as acetic acid but it was also negatively correlated with TNF- α (serum and tibia). Iso-butyric acid was negatively correlated with IL-1B (ceca), IL-18 (serum), and TNF- α (serum and tibia) and positively correlated with IL-10 (serum). Iso-valeric acid was negatively correlated with IL-1B (ceca) and positively correlated with IL-10 (serum and ceca) and ZO-1 Claudin-1 as shown in the figure 5 (i).

**Correlation between SCFA's, Tibia microstructure and Bone Markers**

Spearman correlation heatmap was performed to demonstrate the correlation between short chain fatty acids, tibia microstructure and bone formation and resorption markers.

On day 15, acetic acid was positively correlated with Tb. Th and BS/BV% and was negatively correlated with Tb.sep and TRAF6. Propionic acid had highly positive correlation with BV/TV, Tb. Th, BS/BV, BV/TV, TS and osteocalcin. Butyric acid and iso-butyric acid also showed the similar trend with regards to tibia microstructure and negatively correlated with Tb. Sep. Iso-butyric was positively correlated with ALP (tibia bone marrow). Iso-valeric acid was highly positively correlated with ALP (tibia and serum) and Tb. N and negatively correlated with TRAP and Tb. Sep. Valeric acid had shown positive correlation with tibia microstructure, osteocalcin and negatively correlation with TRAF6 as shown in the figure 5(j).

On day 30, Acetic acid was positively correlated with bone mineral density (BMD) and negatively correlated with bone resorption markers TRAP and NFATC1. Propionic acid was positively correlated with Tb.N and negatively correlated with TRAP (indicator of osteoclasts). Butyric acid had a positive correlation with BMD, tibia microstructure, ALP (Tibia) and negative correlation with NFATC1. Iso-butyric acid was extremely highly positive correlated with BMD, positively correlated with tibia microstructure and negatively correlated with Tb.sep and NFATC1. Iso-valeric acid was highly positive correlated with Tb. Th and osteocalcin (tibia) and extremely highly negatively correlated with TRAP. Valeric acid was positively correlated with BMD, ALP and had extreme high negative correlation with NFATC1 as shown in the figure 5(k).

On day 60, Acetic acid had extremely highly positive correlation with BMD and negative correlation with Tb. Sep. and NFATC1. Propionic acid was positively correlated with BMD and Tb. N and negatively correlated with Tb. Sep., NFATC-1 and TRAF-6. Butyric acid was positively correlated with BS/BV and highly negatively correlated with TRAF6. Iso-butyric acid and iso-valeric had a positive correlation with Tibia microstructure and bone formation maker (ALP). Valeric acid had high positive correlation with BV/TV, TS, BS/BV, Tb. Th, bone formation markers (ALP and osteocalcin) and negatively correlation with TRAP as shown in the figure 5(l).

**Effects of perennial ryegrass on gene expression related to bone formation and resorption**

LPS, a potent endotoxin produced by Gram-negative bacteria such as *Escherichia coli*, plays a crucial role in triggering systemic inflammation and bone resorption. In the commercial feeding group (CD), the relative abundance of *E. coli* was significantly higher, leading to increased LPS production and its synthesizing genes in the cecum leading to the activation of Toll like receptors (Table 1). In contrast, ryegrass intake in the GD group significantly reduced *E. coli* abundance and downregulated the expression of key LPS synthesis genes (rfaL, rfaK). This reduction in LPS production contributed to decreased TLR-4 activation and lower systemic inflammation. Pro-inflammatory cytokines play an important role in systemic inflammation. We measured the mRNA expression of IL-1B, IL-18 and TNF-α ceca and tibia. IL-1B and TNF-α had significantly higher ($P<0.01$) mRNA expression both in ceca and tibia on day 15, 30 and 60. IL-18 had also significantly higher ($P<0.01$) mRNA expression both in ceca and tibia on day 15, 30 and also on day 60 ($P<0.05$). IL-10 is known be an anti-inflammatory cytokine reducing the systemic inflammation. Ryegrass intake groups (GD) showed significantly higher ($P<0.01$) mRNA expression of IL-10 both in ceca and tibia (Table 1). Body antioxidant system plays an important role in bone homeostasis through redox signaling (NrF2/Keap1) pathways. The mRNA expression level of NrF2 showed a significant difference ($P<0.01$) between the two groups. Ryegrass improved the antioxidant status of the GD by the increasing the expression level of NrF2 and reducing the expression of Keap1 (major gene responsible for ROS activation).

We observed the changes in the tibial growth plate as a result of inflammatory responses and that mRNA expression levels of HIF-1 and VEGFA in tibial growth plates were significantly lower in ($P<0.01$) on day 15, 30 and on day 60 ($P<0.05$) in CD groups (Table 1). PMCA1b, CaBP-D28, NPt2a and NPt2b are the calcium and phosphorus transporters. The duodenal mRNA expression of PMCA1b, NPt2a and NPt2a were significantly increased ($P<0.01$) GD group On Day 15 and 30. On day 60, mRNA PMCA1b ($P<0.05$) and mRNA NPt2b ($P<0.01$) relative expression levels were also increased as a result of ryegrass intake. CaBP-D28 mRNA expression level was significantly higher ($P<0.01$) in GD group on day 30 and 60 as

shown in Table 1. ALP and TRAP are the bone markers responsible for bone formation and bone resorption in the tibia. The mRNA expression level of ALP in the tibia was significantly higher (P<0.01) in GD group on day 15, 30 and also on day 60 (P<0.05). The Wnt/B-catenin pathway plays a crucial role in bone formation by regulating the osteoblastogenesis and bone mass. Wnt-10b signaling regulates the expression of osteogenic genes such as RUNX, SOST and OCN. Wnt-10b signaling also regulates the SMAD pathway and it's regulating genes (ALP, OPG and TGF-B) responsible for bone formation. The mRNA expression of osteogenic pathways such as Wnt10b and SMAD was significantly higher (P<0.01) in GD group as compared to CD groups (Table 1). On day 15, the genes regulating these pathways such as SOST, OCN, OPG and TGF-B had significantly higher (P<0.01) mRNA expression levels as a result of ryegrass intake. On Day 30, same trend was followed in GD groups including RUNX2. On Day 60, RUNX2 (P<0.01); SOST, OCN, OPG, and TGF-B had significantly higher (P<0.01) mRNA levels in the tibia in GD groups as compared to CD group. The mRNA expression of local bone derived regulators showed a significant difference between the commercial and ryegrass intake groups. At day 15, 30 and 60, the mRNA expression levels of these local bone regulators (FGF23, PHEX, DMPI and MEPE) were significant higher (P<0.01) in GD group as compared to CD groups. GPR43, GPR41 and GPR109a have been identified as receptors for SCFA's, the molecular mechanisms underlying the role of SCFA's in bone health have elucidated. These 3 receptors (GPR41, GPR 43, GPR109a) showed significantly higher (P<0.01) mRNA expression in ceca as a result of ryegrass feeding on day 15 and 30. Generated by the goblets cells, MUC-2 is the major constituent of intestinal mucus layer. Inhibition of Notch pathway can result in a conversion of epithelial cells into goblet cells. Compared with CD, the number of goblet cells and MUC-2 mRNA expression in the ceca showed significant difference (P<0.01) in GD group. In addition, the mRNA expression level of Notch1 and Notch2 were significantly downregulated as a result of ryegrass intake in GD group indicating the enhanced level of MUC-2 leading to efficient conversion of IEC into GC. NF-κB plays a very crucial role in bone resorption by increasing the inflammatory response. The genes responsible for bone resorption due to LPS induced inflammatory response are RANKL, MyD88, NFATC-1, TRAF-6 and HDAC playing an important role in NF-κB regulation. Ryegrass intake significantly reduced the mRNA expression of NF-κB on day 30 and 60. RANKL and TRAF6 were also downregulated on day 15, 30 and 60 as a result of ryegrass feeding. GD group had significantly lower mRNA expression levels of NFATC-1, MyD88 and HDAC (P<0.01) on all three phases as compared to CD group (Table 1).

**Protein Expression genes related to bone formation and resorption**

Western Blotting was performed at 60$^{th}$ day of the experiment. The protein expression of Wnt10b and its regulating genes (RUNX2, OCN, SMAD, ALP and OPG) were significantly higher (P<0.01) in GD group as compared to GD group resulting in active bone formation (Figure 7s). The protein expression of NF-κB and its regulating genes (RANKL, NFATC-1 and HDAC) were significantly higher in commercial feeding group (CD) as compared to ryegrass intake group (Figure 7t). The protein expression of calcium (CaBP-28K, PMCA1b) and Phosphorus transporters (NPt2a) were significantly higher (P<0.01) in GD group (Figure 7u). Ryegrass intake had also significantly increased (P<0.01) the protein expression of local bone derived regulators (PHEX, FGF-23) as compared to commercial feeding. Protein expression of angiogenic genes were also performed to observe the blood vessel formation rate. The protein expression of the angiogenic genes (HIF-1 and VEGFA) were also significantly higher (P<0.01) as a result of ryegrass intake (Figure 7v).

**Immunofluorescence analysis of NF-κB and Wnt10b**

To further confirm the activation of NF-κB and Wnt10b in the tibia of meat geese, the nuclear translocation of these two signaling pathway genes by the immunofluorescence was performed. As observed via using confocal fluorescence microscope, most of the NF-κB protein was translocated in the cell nucleus in the tibia of the meat geese in CD group as compared to GD group (Figure 8a). To evaluate the impact of ryegrass intake on bone formation pathways, the nuclear translocation of Wnt10b was also determined by immunofluorescence analysis (Figure 8b). The results revealed increased Wnt10b in GD group as compared to CD group suggesting that ryegrass intake may involve actively in bone formation.

**Discussion**

Goose body weight was affected by the addition of ryegrass. There was no significant difference between body and feed intake on day 15. ADG, ADFI and FCR were significantly lower in the GD group as compared to the CD group on day 30 and 60 as a result of lower solid feed consumption due to pasture intake. In this study, ADG, ADFI and F:G ratio were significantly decreased in Ryegrass grazing group (GD). The results of this study regarding ADG was also in line with study of (Ali et al., 2022a). We speculate that this may be due to the lower energy content of the ryegrass which reduces the ADG of the wanpu geese.

There was a significant increase in tibial length as a result of commercial feeding (CD). There was no significant difference in tibia width between the two groups. These results were in line with study of (Mendoza-Ávila et al., 2020). Dietary fiber consumption has been linked to improve glucose regulation and enhance skeletal muscle function. These findings suggest that dietary fiber intervention may serve as a nutritional strategy to mitigate the age related reduction in bone mass and muscular strength, promoting better metabolic and musculoskeletal health.

There was no significant difference in serum Ca level between the groups. However, Ca content in the tibia were significantly higher in GD group. These observations were in line with the study of (Jakeman et al., 2016). Dietary fiber supplementation resulted in increased bone calcium retention in geese, leading to enhanced bone calcium balance. There was significant increase in serum, tibia P and tibia ash content in GD group as a result of Ryegrass feeding which probably increased the intestinal phosphorus transport by upregulating the gene expression of *NaPiIIb* (potent intestinal P-transporter). Similar findings broiler chicken studies suggest that significant drop in GIT pH resulted in optimized ileal nutrient digestibility and improved P utilization, contributing to better mineral absorption and bone health (Y.C. Chen and T.C. Chen ., 2004).

There was a significant improvement in tibia microstructure as a result of ryegrass intake. BMD, BV, BV/TV, TS, Tb. N were significantly improved in GD as compared to CD group in both trabecular and cortical section. GD had significantly lower Tb.sp. compared with commercial feeding. These results were in line with study of (Johnson et al., 2011; Zhang et al., 2021). A possible reason for increased bone mineralization and improved tibia microstructure is through direct effect of SCFA's produced through fermentation of dietary fiber from the ryegrass intake. Osteocytes represent the predominant cell type found within the mineralized matrix of bone tissue. They play a crucial role in mechanosensing and are instrumental in regulating the activities of both osteoclasts and osteoblasts, in addition to facilitating the process of bone mineralization. Their exact contributions to these processes are complex and may vary depending on the physiological context. Phex, Dmp-1, and Mepe are among the genes that are highly expressed in osteocytes and are crucial for the processes of bone mineralization and the maintenance

of mineral homeostasis (Robling and Bonewald, 2020). These results suggest that the impact of Ryegrass consumption on bone health is probably facilitated by osteocytes. Ryegrass intake upregulated mRNA expression of these local bone derived regulators. Our findings showed increased expression of *Mepe* and *Dmp-1* with ryegrass feeding. While *Mepe* functions as an inhibitor of bone crystal formation, its interaction with *Phex* forms a complex that mitigates its inhibitory effects (Staines et al., 2012). Furthermore, elevated *Dmp-1*, a key regulator of hydroxyapatite nucleation, suggests a coordinated effort by osteocytes to modulate bone mineralization, ensuring balance in the mineralization process. These molecular changes highlight an adaptive dietary response to regulate bone health (Narayanan et al., 2003).

Ryegrass intake has been shown to have its proven anti-inflammatory effects both vivo and in vitro (Ali et al., 2022a), believing its potential to inhibit bone resorption. ALP supports bone calcification by hydrolyzing phosphate esters, while sodium butyrate enhances osteogenesis by upregulating ALP and osteoblast markers (Lee et al., 2006). In the present study, the GD diet reduced the serum TRAP, tibia NFATC-1 and TRAF-6 (markers of bone resorption) and increased the level of serum and tibia ALP and OCN (markers of bone formation) suggesting that ryegrass supplementation downregulates bone resorption. This was supported by a previous study of (Tang et al., 2020). These results support the idea that ryegrass may offer therapeutic benefits for bone health, as indicated by both in vitro and in vivo studies.

The body's intrinsic immune defense mechanism is triggered by the assault of reactive oxygen species (ROS), which subsequently activates the NF-κB signaling pathway and augments the Keap1-Nrf2 pathway (Suzuki and Yamamoto, 2017). It is well known that enhanced Nrf2 regulation is expected to support antioxidant defense mechanisms. We found that meat geese at 15, 30, and 60 days showed increased levels of antioxidants such CAT (Catalase) and GSH-PX in response to Ryegrass feeding. We conducted an evaluation of the oxidative mediator malondialdehyde (MDA) to determine the role of antioxidants in mitigating the mediators responsible for reactive oxygen species (ROS) damage in CD and GD groups at 15, 30, and 60 days. Our findings indicated a significant increase in MDA levels in the CD meat geese in comparison to the GD meat geese. These findings suggest that ryegrass feeding effectively activates antioxidant mechanisms, likely through the modulation of the NF-κB and Keap1-Nrf2 pathways, thereby reducing ROS-induced damage and supporting overall cellular protection.

Calcium-regulating hormones are crucial for bone health: PTH is responsible for maintenance of calcium levels and bone turnover, Vitamin D3 enhances calcium and phosphorus absorption and affects bone directly, while calcitonin inhibits bone resorption and prevents hypercalcemia. Estrogen being a potent regulator of bone remodeling process, acts on both osteoclasts and osteoblasts (Emmanuelle et al., 2021). IGF-1 is a critical mediator of bone and most abundant growth factor deposited in bone matrix (Xian et al., 2012). IGF-1 promotes the development of long bone, their maturation resulting in better bone mass (Locatelli and Bianchi, 2014). We observed a marked increase in Estrogen, vitamin $D_3$, IGF-1 and calcitonin in the GD group. These findings were in line with (Monroe et al., 2007). Ryegrass intake significantly reduced the serum serotonin and PTH levels as compared to commercial feeding (CD). Maintaining optimal bone health necessitates a complex interaction among various hormones, each playing a distinct role in sustaining bone integrity. These hormones are instrumental

in balancing the processes of bone formation and resorption, regulating calcium levels, and ensuring the skeletal system remains robust and resilient.

Recent findings have proved the significant role of dietary fiber on gut microbiota in geese (Ali et al., 2022b). Ryegrass feeding by meat geese was associated with mechanisms that simultaneously inhibit bone loss by mitigating systemic inflammation. As a result, the novel characteristic of Ryegrass grazing as a source of high dietary fiber lies in its ability to establish a pathway-based mechanism that enhances the prevalence of intestinal bacteria associated with bone formation, while simultaneously inhibiting the proliferation of lipopolysaccharide (LPS)-producing bacteria, particularly Escherichia coli. These changes enhance nutrient absorption, strengthen the mucus layer, and reduce LPS production and gut permeability. Gut microbial diversity of the meat geese was significantly altered by ryegrass intake. In the present study, wanpu geese were dominantly occupied by *Firmicutes* and B*acteriodetes. Bacteriodetes* are associated with cellulose degradation (Berry, 2016). We found that *Bacteriodetes* increased with ryegrass intake. *Firmicutes*, an important phylum, is involved in protein and fat metabolism (Okazaki et al., 2016). Our results showed *Firmicutes* were decreased as a result of ryegrass intake because commercial diet contained more calories. Concurrently, the relative abundance of *Bacteriodetes* increased with dietary fiber intake (El Kaoutari et al., 2013). There was significant reduction *Firmicutes:Bacteriodetes* ratio in GD group. These findings were in line with (Guo et al., 2019) providing the evidence that that reduced *Firmicutes/Bacteroidetes* ratio was associated with reduction in bone loss. B-diversity was significantly improved in GD group. Ryegrass intake increased the relative abundance of SCFA's producing bacteria responsible for bone homeostasis. It is possible that *Firmicutes/Bacteroidetes* ratio might serve as a critical mediators influencing tibia properties in meat geese.

An additional mechanism through which Ryegrass may positively influence bone health is microbial metabolites production, specifically short-chain fatty acids and their receptors upregulations (GPR41 and GPR43). FOS (a prebiotic fiber) is linked with an increase in BMD, leading to improved Ca absorption (Takahara et al., 2000). Similarly, in our study, the positive effects of Ryegrass improved the tibia microstructure in conjunction with SCFAs (acetate, propionate, and *n*-butyrate) through its prebiotic effects. Butyrate and propionate can modulate the metabolic pathways of pre-osteoclasts differentiation, driving a shift toward glycolytic metabolism. This metabolic reprogramming induces cellular stress, which subsequently impairs osteoclast differentiation (Lucas et al., 2018). Furthermore, SCFAs may mitigate both intestinal and systemic inflammation, significantly contributing to the bone metabolism maintenance (Zaiss et al., 2019), which was further advocated by our findings. Ryegrass exerts beneficial effects on bone health through its prebiotic influence, promoting the production of SCFAs. These SCFAs enhance tibia microstructure, regulate osteoclast differentiation via metabolic reprogramming, and mitigate inflammation, thereby supporting bone metabolism and maintaining bone mineral density.

Poultry require a specific quantity of dietary fiber to facilitate optimal intestinal physiological functions. The intestinal villi serve as the principal location for nutrient absorption, and the efficiency of nutrient absorption and utilization is contingent upon the development of this anatomical structure (Sklan et al., 2003). Ryegrass intake significantly increased the VH, VW, VSA, VH/CD of the ileum and mucosal and muscularis thickness of the caecum as compared to CD group. These findings were in agreement of (Tejeda and Kim, 2021) demonstrating that an 8% crude fiber level diet with soybean hulls as the fiber source could significantly increase the villus height of the duodenum, jejunum and ileum of broilers.

Ryegrass also enhanced the ceca Goblet cells production significantly in GD group. These findings were in line with (Ali et al., 2022a).

Reactive oxygen species (ROS) induce apoptosis in osteoblasts and osteocytes, facilitating the process of osteoclastogenesis (Almeida et al., 2007). These events increase the rate of bone remodeling, consequently altering and diminishing bone mass. Several factors that regulate the activity of osteoclasts and osteoblasts, and consequently influence bone remodeling, include the ligand of receptor activator of NF-κB (RANKL) and osteoprotegerin (OPG). By interacting with certain receptors in preostoeclasts, RANKL promotes osteoclastogenesis and bone resorption activating osteoclast differentiation and activity. On the other hand, OPG, which is generated through the Wnt/βcatenin signaling pathway, is a soluble receptor that may bind to and block RANKL, which decreases the activity of osteoclasts (Jilka et al., 2013). The balance between bone formation and resorption is maintained by controlling the levels of the RANKL/OPG ratio. It can be concluded from this study that Wnt pathway regulates $Nrf_2$ signaling through a KEAP1-independent manner promoting bone formation in meat geese.

Inflammation serves as a crucial defense mechanism in organisms, protecting against external damage. A significant biological contributor to inflammation is the pathogenic bacterium Escherichia coli (E. coli), which exerts a pronounced impact in this context. Various chronic inflammatory conditions are associated with bone health, particularly influencing the metabolism of calcium (Ca) and phosphorus (P), ultimately leading to a decrease in bone formation. Pro-inflammatory cytokines, such as IL-18, IL-1β, and TNF-α, impede bone growth through their interactions. These inflammatory mediators counteract the effects of growth hormone, with the NF-κB signaling pathway being particularly influential. The activation of NF-κB facilitates osteoclastogenesis while simultaneously inhibiting osteoblastogenesis (Iotsova et al., 1997). An intact intestinal barrier is essential for immune defense, and increased serum levels of diamine oxidase (DAO) may serve as a marker of intestinal dysfunction or permeability. There was also the negative impact of LPS production compromising the immune system. Ryegrass intake significantly reduced the production of inflammatory Cytokines (IL-1 β, IL-18, TNF-α), LPS production and increased the production of anti-inflammatory cytokine (IL-10) serum, ceca and tibia. Serum DAO level was significantly lower in GD group as compared to CD group. Ryegrass intake significantly upregulated the levels of Tight junction proteins. These findings were in agreement with the study of (Ali et al., 2022a). In the present study, the levels of IL-1β, IL-18 and TNF-α, were elevated in the CD group as a results of increased LPS production and E.coli growth. There was no doubt that LPS elicited a vigorous immune response in the ceca. It should be noted that Ryegrass intake increased the level of IL-10 in the serum, tibia and ceca. Our findings suggest that the consumption of ryegrass may play a role in the differentiation of T helper (Th) cells into $Th_2$-type and regulatory T (Treg) cells.

Despite the Ryegrass-mediated improvement in tibia microstructure and bone mass, Wnt-10b is an important molecular pathway through it promotes bone formation and prevents bone resorption. Wnt10b induces osteoblast differentiation in vitro (Cawthorn et al., 2012). The role of Wnt10b for bone mass is further demonstrated by the observation that global deletion of the Wnt10b gene results in a decreased amount of trabecular bone (Stevens et al., 2010). In the present study, Ryegrass intake significantly upregulated the expression of Wnt10b and also the genes (RUNX-2, SOST, OCN, BMP2) regulating it. These results were in line with study of (Islam et al., 2024) promoting bone formation as a result of ryegrass intake. The mRNA expression of NF-κB and its regulating genes were significantly downregulated in GD group. Therefore, these results suggest that ryegrass decreased inflammatory bone loss which might be due to NF-κB signaling inactivation. Similar findings were observed in the study of (Zhang et al., 2022).

In conclusion, supplementing ryegrass advocates the significant potential for mitigating the bone loss by positively influencing the gut health and modulating Wnt10b/ NF-κB signaling pathway. Dietary ryegrass contributes to the maintenance of balanced gut microbiota facilitating the production of SCFAs. SCFAs enhance the mineral absorption by reducing the systemic inflammation. This balance ultimately supports the bone integrity by modulating the immune response. Furthermore, ryegrass appears to stimulate the Wnt10b pathway, which promotes the differentiation of osteoblasts, while concurrently inhibiting the NF-κB responsible for inflammatory bone loss. Collectively, these findings indicate that ryegrass feeding represents a promising dietary strategy for enhancing bone health in meat geese through modulation of gut microbiota and key signaling pathways.

## Acknowledgements

We thank Henan Daidai goose Agriculture and Animal husbandry development Co. LTD (Zhumadian, China) for providing Wanfu meat geese stocks used in this study. This work was financially supported by the Science and Technology Innovation Leading Talent in Central Plains (No. 244200510010) China Agriculture Research System of MOF and MARA (No. CARS-34), the Science and Technology Innovation Team of Henan Province High Quality Forage and Animal Health (No. 22IRTSTHN022).

## REFERENCES


Y.C.C., T.C.C., 2004. Mineral Utilization in Layers as Influenced by Dietary Oligofructose and Inulin. Intl. J. Poult. Sci. 3, 442–445. https://doi.org/10.3923/ijps.2004.442.445

Ali, Q., Ma, S., Farooq, U., Niu, J., Li, F., Li, D., Wang, Z., Sun, H., Cui, Y., Shi, Y., 2022a. Pasture intake protects against commercial diet-induced lipopolysaccharide production facilitated by gut microbiota through activating intestinal alkaline phosphatase enzyme in meat geese. Front. Immunol. 13, 1041070. https://doi.org/10.3389/fimmu.2022.1041070

Ali, Q., Ma, S., La, S., Guo, Z., Liu, B., Gao, Z., Farooq, U., Wang, Z., Zhu, X., Cui, Y., Li, D., Shi, Y., 2022b. Microbial short-chain fatty acids: a bridge between dietary fibers and poultry gut health — A review. Anim. Biosci. 35, 1461–1478. https://doi.org/10.5713/ab.21.0562

Almeida, M., Han, L., Martin-Millan, M., Plotkin, L.I., Stewart, S.A., Roberson, P.K., Kousteni, S., O'Brien, C.A., Bellido, T., Parfitt, A.M., Weinstein, R.S., Jilka, R.L., Manolagas, S.C., 2007. Skeletal Involution by Age-associated Oxidative Stress and Its Acceleration by Loss of Sex Steroids. J. biol. chem. 282, 27285–27297. https://doi.org/10.1074/jbc.M702810200

Berry, D., 2016. The emerging view of Firmicutes as key fibre degraders in the human gut. Environ. Microbiol. 18, 2081–2083. https://doi.org/10.1111/1462-2920.13225

Cawthorn, W.P., Bree, A.J., Yao, Y., Du, B., Hemati, N., Martinez-Santibañez, G., MacDougald, O.A., 2012. Wnt6, Wnt10a and Wnt10b inhibit adipogenesis and stimulate osteoblastogenesis through a β-catenin-dependent mechanism. Bone 50, 477–489. https://doi.org/10.1016/j.bone.2011.08.010

Chilibroste, P., Tamminga, S., Boer, H., Gibb, M.J., Den Dikken, G., 2000. Duration of Regrowth of Ryegrass (Lolium perenne) Effects on Grazing Behavior, Intake, Rumen Fill, and Fermentation of Lactating Dairy Cows. J. Dairy Sci. 83, 984–995. https://doi.org/10.3168/jds.S0022-0302(00)74963-0

Choi, K.-C., Son, Y.-O., Hwang, J.-M., Kim, B.-T., Chae, M., Lee, J.-C., 2017. Antioxidant, anti-inflammatory and anti-septic potential of phenolic acids and flavonoid fractions isolated from *Lolium multiflorum*. Pharm. Biol. 55, 611–619. https://doi.org/10.1080/13880209.2016.1266673

D'Amelio, P., Sassi, F., 2018. Gut Microbiota, Immune System, and Bone. Calcif. Tissue Int. 102, 415–425. https://doi.org/10.1007/s00223-017-0331-y

David, L.S., Abdollahi, M.R., Bedford, M.R., Ravindran, V., 2022. Requirement of digestible calcium at different dietary concentrations of digestible phosphorus for broiler chickens. 2. Broiler growers (d 11 to 24 post-hatch). Poult. Sci. 101, 102135. https://doi.org/10.1016/j.psj.2022.102135

Die, L., Yan, P., Jun Jiang, Z., Min Hua, T., Cai, W., Xing, L., 2012. Glycogen synthase kinase-3 beta inhibitor suppresses Porphyromonas gingivalis lipopolysaccharide-induced CD40 expression by inhibiting nuclear factor-kappa B activation in mouse osteoblasts. Mol. Immunol. 52, 38–49. https://doi.org/10.1016/j.molimm.2012.04.005

Dobrowolski, P., Tomaszewska, E., Muszyński, S., Blicharski, T., Pierzynowski, S.G., 2017. Dietary 2-oxoglutarate prevents bone loss caused by neonatal treatment with maximal dexamethasone dose. Exp. Biol. Med. (Maywood) 242, 671–682. https://doi.org/10.1177/1535370217693322

El Kaoutari, A., Armougom, F., Gordon, J.I., Raoult, D., Henrissat, B., 2013. The abundance and variety of carbohydrate-active enzymes in the human gut microbiota. Nat. Rev. Microbiol. 11, 497–504. https://doi.org/10.1038/nrmicro3050

Emmanuelle, N.-E., Marie-Cécile, V., Florence, T., Jean-François, A., Françoise, L., Coralie, F., Alexia, V., 2021. Critical Role of Estrogens on Bone Homeostasis in Both Male and Female: From Physiology to Medical Implications. Int. J. Mol. Sci. 22, 1568. https://doi.org/10.3390/ijms22041568

Guo, B., Li, D., Zhou, B., Jiang, Y., Bai, H., Zhang, Y., Xu, Q., Zhao, W., Chen, G., 2019. Comparative characterization of bacterial communities in geese consuming of different proportions of ryegrass. PLoS One 14, e0223445. https://doi.org/10.1371/journal.pone.0223445

Iotsova, V., Caamaño, J., Loy, J., Yang, Y., Lewin, A., Bravo, R., 1997. Osteopetrosis in mice lacking NF-κB1 and NF-κB2. Nat. Med. 3, 1285–1289. https://doi.org/10.1038/nm1197-1285

Islam, P., Ice, J.A., Alake, S.E., Adedigba, P., Hatter, B., Robinson, K., Clarke, S.L., Ford Versypt, A.N., Ritchey, J., Lucas, E.A., Smith, B.J., 2024. Fructooligosaccharides act on the gut–bone axis to improve bone independent of Tregs and alter osteocytes in young adult C57BL/6 female mice. JBMR Plus 8, ziae021. https://doi.org/10.1093/jbmrpl/ziae021

Jakeman, S.A., Henry, C.N., Martin, B.R., McCabe, G.P., McCabe, L.D., Jackson, G.S., Peacock, M., Weaver, C.M., 2016. Soluble corn fiber increases bone calcium retention in postmenopausal women in a dose-dependent manner: a randomized crossover trial. Am. J. Clin. Nutr. 104, 837–843. https://doi.org/10.3945/ajcn.116.132761

Jilka, R.L., Noble, B., Weinstein, R.S., 2013. Osteocyte apoptosis. Bone 54, 264–271. https://doi.org/10.1016/j.bone.2012.11.038

Johnson, C.D., Lucas, E.A., Hooshmand, S., Campbell, S., Akhter, M.P., Arjmandi, B.H., 2011. Addition of Fructooligosaccharides and Dried Plum to Soy-Based Diets Reverses Bone Loss in the Ovariectomized Rat. eCAM. 2011, 836267. https://doi.org/10.1093/ecam/nen050

Jones, T.A., Dawkins, M.S., 2010. Environment and management factors affecting Pekin duck production and welfare on commercial farms in the UK. Br. Poult. Sci. 51, 12–21. https://doi.org/10.1080/00071660903421159

Karakan, T., Tuohy, K.M., Janssen-van Solingen, G., 2021. Low-Dose Lactulose as a Prebiotic for Improved Gut Health and Enhanced Mineral Absorption. Front. Nutr. 8, 672925. https://doi.org/10.3389/fnut.2021.672925

Korver, D.R., 2023. Review: Current challenges in poultry nutrition, health, and welfare. Animal 17, 100755. https://doi.org/10.1016/j.animal.2023.100755

Lee, H.W., Suh, J.H., Kim, A.Y., Lee, Y.S., Park, S.Y., Kim, J.B., 2006. Histone Deacetylase 1-Mediated Histone Modification Regulates Osteoblast Differentiation. Mol. Endocrinol. 20, 2432–2443. https://doi.org/10.1210/me.2006-0061

Li, Y., Zhang, H., Chen, Y.P., Yang, M.X., Zhang, L.L., Lu, Z.X., Zhou, Y.M., Wang, T., 2015. Bacillus amyloliquefaciens supplementation alleviates immunological stress in lipopolysaccharide-challenged broilers at early age. Poult. Sci. 94, 1504–1511. https://doi.org/10.3382/ps/pev124

Liu, J., Xiao, Q., Xiao, J., Niu, C., Li, Y., Zhang, X., Zhou, Z., Shu, G., Yin, G., 2022. Wnt/β-catenin signalling: function, biological mechanisms, and therapeutic opportunities. Sig. Transduct. Target. Ther. 7, 3. https://doi.org/10.1038/s41392-021-00762-6

Livak, K.J., Schmittgen, T.D., 2001. Analysis of Relative Gene Expression Data Using Real-Time Quantitative PCR and the 2−ΔΔCT Method. Methods 25, 402–408. https://doi.org/10.1006/meth.2001.1262

Locatelli, V., Bianchi, V.E., 2014. Effect of GH/IGF-1 on Bone Metabolism and Osteoporsosis. Int. J. Endocrinol. 2014, 235060. https://doi.org/10.1155/2014/235060

Lorenzo, J., Horowitz, M., Choi, Y., 2008. Osteoimmunology: Interactions of the Bone and Immune System. Endocr. Rev. 29, 403–440. https://doi.org/10.1210/er.2007-0038

Lucas, S., Omata, Y., Hofmann, J., Böttcher, M., Iljazovic, A., Sarter, K., Albrecht, O., Schulz, O., Krishnacoumar, B., Krönke, G., Herrmann, M., Mougiakakos, D., Strowig, T., Schett, G., Zaiss, M.M., 2018. Short-chain fatty acids regulate systemic bone mass and protect from pathological bone loss. Nat. Commun. 9, 55. https://doi.org/10.1038/s41467-017-02490-4

Ma, B., Hottiger, M.O., 2016. Crosstalk between Wnt/β-Catenin and NF-κB Signaling Pathway during Inflammation. Front. Immunol. 7. https://doi.org/10.3389/fimmu.2016.00378

Mendoza-Ávila, M., Gutiérrez-Cortez, E., Quintero-García, M., Real, A.D., Rivera-Muñoz, E.M., Ibarra-Alvarado, C., Rubio, E., Jiménez-Mendoza, D., Rojas-Molina, I., 2020. Calcium Bioavailability in the Soluble and Insoluble Fibers Extracted from Opuntia ficus indica at Different Maturity Stages in Growing Rats. Nutrients 12, 3250. https://doi.org/10.3390/nu12113250

Monroe, K.R., Murphy, S.P., Henderson, B.E., Kolonel, L.N., Stanczyk, F.Z., Adlercreutz, H., Pike, M.C., 2007. Dietary fiber intake and endogenous serum hormone levels in naturally postmenopausal Mexican American women: the Multiethnic Cohort Study. Nutr. Cancer 58, 127–135. https://doi.org/10.1080/01635580701327935

Narayanan, K., Ramachandran, A., Hao, J., He, G., Park, K.W., Cho, M., George, A., 2003. Dual functional roles of dentin matrix protein 1. Implications in biomineralization and gene transcription by activation of intracellular Ca2+ store. J. Biol. Chem. 278, 17500–17508. https://doi.org/10.1074/jbc.M212700200

Okazaki, Y., Sekita, A., Chiji, H., Kato, N., 2016. Consumption of lily bulb modulates fecal ratios of firmicutes and bacteroidetes phyla in rats fed a high-fat diet. Food Sci. Biotechnol. 25, 153–156. https://doi.org/10.1007/s10068-016-0112-9

Oke, O.E., Akosile, O.A., Oni, A.I., Opowoye, I.O., Ishola, C.A., Adebiyi, J.O., Odeyemi, A.J., Adjei-Mensah, B., Uyanga, V.A., Abioja, M.O., 2024. Oxidative stress in poultry production. Poult. Sci. 103, 104003. https://doi.org/10.1016/j.psj.2024.104003

Rath, N.C., Huff, G.R., Huff, W.E., Balog, J.M., 2000. Factors Regulating Bone Maturity and Strength in Poultry. Poult. Sci. 79, 1024–1032. https://doi.org/10.1093/ps/79.7.1024

Riesenfeld, A., 1972. Metatarsal robusticity in bipedal rats. Am. J. Phys. Anthropol. 36, 229–233. https://doi.org/10.1002/ajpa.1330360211

Robling, A.G., Bonewald, L.F., 2020. The Osteocyte: New Insights. Annu. Rev. Physiol. 82, 485–506. https://doi.org/10.1146/annurev-physiol-021119-034332

Seely, K.D., Kotelko, C.A., Douglas, H., Bealer, B., Brooks, A.E., 2021. The Human Gut Microbiota: A Key Mediator of Osteoporosis and Osteogenesis. Int. J. Mol. Sci. 22, 9452. https://doi.org/10.3390/ijms22179452

Sklan, D., Smirnov, A., Plavnik, I., 2003. The effect of dietary fibre on the small intestines and apparent digestion in the turkey. Br. Poult. Sci. 44, 735–740. https://doi.org/10.1080/00071660310001643750

Smith, P.M., Howitt, M.R., Panikov, N., Michaud, M., Gallini, C.A., Bohlooly-Y, M., Glickman, J.N., Garrett, W.S., 2013. The microbial metabolites, short-chain fatty acids, regulate colonic Treg cell homeostasis. Science 341, 569–573. https://doi.org/10.1126/science.1241165

Song, B., Tang, D., Yan, S., Fan, H., Li, G., Shahid, M.S., Mahmood, T., Guo, Y., 2021. Effects of age on immune function in broiler chickens. J. Anim. Sci. biotechnol. 12, 42. https://doi.org/10.1186/s40104-021-00559-1

Staines, K.A., MacRae, V.E., Farquharson, C., 2012. The importance of the SIBLING family of proteins on skeletal mineralisation and bone remodelling. J. Endocrinol. 214, 241–255. https://doi.org/10.1530/JOE-12-0143

Stevens, J.R., Miranda-Carboni, G.A., Singer, M.A., Brugger, S.M., Lyons, K.M., Lane, T.F., 2010. *Wnt10b* deficiency results in age-dependent loss of bone mass and progressive reduction of mesenchymal progenitor cells. J. Bone Miner. Res. 25, 2138–2147. https://doi.org/10.1002/jbmr.118

Suzuki, T., Yamamoto, M., 2017. Stress-sensing mechanisms and the physiological roles of the Keap1–Nrf2 system during cellular stress. J. Biol. Chem. 292, 16817–16824. https://doi.org/10.1074/jbc.R117.800169

Takahara, S., Morohashi, T., Sano, T., Ohta, A., Yamada, S., Sasa, R., 2000. Fructooligosaccharide Consumption Enhances Femoral Bone Volume and Mineral Concentrations in Rats. J. Nutr. 130, 1792–1795. https://doi.org/10.1093/jn/130.7.1792

Tang, X., Ma, S., Li, Y., Sun, Y., Zhang, K., Zhou, Q., Yu, R., 2020. Evaluating the Activity of Sodium Butyrate to Prevent Osteoporosis in Rats by Promoting Osteal GSK-3β/Nrf2 Signaling and Mitochondrial Function. J. Agric. Food Chem. 68, 6588–6603. https://doi.org/10.1021/acs.jafc.0c01820

Tejeda, O.J., Kim, W.K., 2021. Effects of fiber type, particle size, and inclusion level on the growth performance, digestive organ growth, intestinal morphology, intestinal viscosity, and gene expression of broilers. Poult. Sci. 100, 101397. https://doi.org/10.1016/j.psj.2021.101397

Tyagi, A.M., Yu, M., Darby, T.M., Vaccaro, C., Li, J.-Y., Owens, J.A., Hsu, E., Adams, J., Weitzmann, M.N., Jones, R.M., Pacifici, R., 2018. The Microbial Metabolite Butyrate Stimulates Bone

Formation via T Regulatory Cell-Mediated Regulation of WNT10B Expression. Immunity 49, 1116-1131.e7. https://doi.org/10.1016/j.immuni.2018.10.013
Wang, N., Hao, Y., Fu, L., 2022. Trimethylamine-N-Oxide Promotes Osteoclast Differentiation and Bone Loss via Activating ROS-Dependent NF-κB Signaling Pathway. Nutrients 14, 3955. https://doi.org/10.3390/nu14193955
Whisner, C.M., Martin, B.R., Nakatsu, C.H., Story, J.A., MacDonald-Clarke, C.J., McCabe, L.D., McCabe, G.P., Weaver, C.M., 2016. Soluble Corn Fiber Increases Calcium Absorption Associated with Shifts in the Gut Microbiome: A Randomized Dose-Response Trial in Free-Living Pubertal Females. J. Nutr. 146, 1298–1306. https://doi.org/10.3945/jn.115.227256
Xian, L., Wu, X., Pang, L., Lou, M., Rosen, C.J., Qiu, T., Crane, J., Frassica, F., Zhang, L., Rodriguez, J.P., Jia, X., Yakar, S., Xuan, S., Efstratiadis, A., Wan, M., Cao, X., 2012. Matrix IGF-1 maintains bone mass by activation of mTOR in mesenchymal stem cells. Nat. Med. 18, 1095–1101. https://doi.org/10.1038/nm.2793
Xu, T., Zheng, J., Jin, W., Li, L., Lin, L., Shaukat, A., Zhang, C., Cao, Q., Ashraf, M., Huang, S., 2022. Total Flavonoids of Rhizoma Drynariae Ameliorate Bone Growth in Experimentally Induced Tibial Dyschondroplasia in Chickens via Regulation of OPG/RANKL Axis. Front. Pharmacol. 13, 881057. https://doi.org/10.3389/fphar.2022.881057
Yamashita, T., Yao, Z., Li, F., Zhang, Q., Badell, I.R., Schwarz, E.M., Takeshita, S., Wagner, E.F., Noda, M., Matsuo, K., Xing, L., Boyce, B.F., 2007. NF-κB p50 and p52 Regulate Receptor Activator of NF-κB Ligand (RANKL) and Tumor Necrosis Factor-induced Osteoclast Precursor Differentiation by Activating c-Fos and NFATc1. J. Biol. Chem. 282, 18245–18253. https://doi.org/10.1074/jbc.M610701200
Yin, H., Huang, J., 2016. Effects of soybean meal replacement with fermented alfalfa meal on the growth performance, serum antioxidant functions, digestive enzyme activities, and cecal microflora of geese. J. Integr. Agric. 15, 2077–2086. https://doi.org/10.1016/S2095-3119(15)61198-4
Zaiss, M.M., Jones, R.M., Schett, G., Pacifici, R., 2019. The gut-bone axis: how bacterial metabolites bridge the distance. J. Clin. Invest. 129, 3018–3028. https://doi.org/10.1172/JCI128521
Zhang, H., Chen, Yanan, Chen, Yueping, Li, Y., Jia, P., Ji, S., Zhou, Y., Wang, T., 2020. Dietary pterostilbene supplementation attenuates intestinal damage and immunological stress of broiler chickens challenged with lipopolysaccharide. J. Anim. Sci. 98, skz373. https://doi.org/10.1093/jas/skz373
Zhang, H., Qin, S., Zhu, Y., Zhang, X., Du, P., Huang, Y., Michiels, J., Zeng, Q., Chen, W., 2022. Dietary Resistant Starch From Potato Regulates Bone Mass by Modulating Gut Microbiota and Concomitant Short-Chain Fatty Acids Production in Meat Ducks. Front. Nutr. 9, 860086. https://doi.org/10.3389/fnut.2022.860086
Zhang, H., Zeng, Q., Bai, S., Wang, J., Ding, X., Xuan, Y., Su, Z., Zhang, K., 2018. Effect of graded calcium supplementation in low-nutrient density feed on tibia composition and bone turnover in meat ducks. Br. J. Nutr. 120, 1217–1229. https://doi.org/10.1017/S0007114518002556
Zhang, Z., Lin, T., Meng, Y., Hu, M., Shu, L., Jiang, H., Gao, R., Ma, J., Wang, C., Zhou, X., 2021. FOS/GOS attenuates high-fat diet induced bone loss via reversing microbiota dysbiosis, high intestinal permeability and systemic inflammation in mice. Metabolism 119, 154767. https://doi.org/10.1016/j.metabol.2021.154767
Zheng, M., Mao, P., Tian, X., Meng, L., 2021. Effects of grazing mixed-grass pastures on growth performance, immune responses, and intestinal microbiota in free-range Beijing-you chickens. Poult. Sci. 100, 1049–1058. https://doi.org/10.1016/j.psj.2020.11.005
Zhong, X., Zhang, F., Yin, X., Cao, H., Wang, X., Liu, D., Chen, J., Chen, X., 2021. Bone Homeostasis and Gut Microbial-Dependent Signaling Pathways. J. Microbiol. Biotechnol. 31, 765–774. https://doi.org/10.4014/jmb.2104.04016

1082

1083 **Table 1.** mRNA expression levels of E.coli, TLR-4, LPS related genes, inflammatory cytokines anti-inflammatory cytokines, redox
1084 signaling genes, angiogenesis genes, Ca and Phosphorus transporters, ALP, WNT-10b and its regulating genes, local bone derived
1085 regulators, SCFA's receptors, MUC-2 and its regulation genes, NF-κB and its regulating genes.

| | | 15d | | | 30d | | | 60d | | |
|---|---|---|---|---|---|---|---|---|---|---|
| **Tissues** | **Gene** | **CD** | **GD** | **P-value** | **CD** | **GD** | **P-value** | **CD** | **GD** | **P-value** |
| **Ceca** | E.coli | 1.00 | 0.32 | P<0.01 | 1.90 | 0.87 | P<0.01 | 2.46 | 1.09 | P<0.01 |
| | TLR-4 | 1.00 | 0.31 | P<0.01 | 1.52 | 1.21 | P<0.05 | 2.00 | 1.36 | P<0.01 |
| | rfaK | 1.00 | 0.25 | P<0.01 | 0.79 | 0.31 | P<0.01 | 0.76 | 0.53 | P<0.05 |
| | rfaL | 1.00 | 0.89 | P>0.05 | 1.14 | 0.48 | P<0.01 | 0.20 | 0.24 | P>0.05 |
| | IL-1B | 1.00 | 0.05 | P<0.01 | 1.62 | 0.08 | P<0.01 | 0.25 | 0.11 | P<0.01 |
| | TNF-α | 1.00 | 0.13 | P<0.01 | 0.95 | 0.23 | P<0.01 | 0.79 | 0.42 | P<0.01 |
| | IL-18 | 1.00 | 0.49 | P<0.01 | 1.03 | 0.36 | P<0.01 | 0.85 | 0.39 | P<0.05 |
| | IL-10 | 1.00 | 1.26 | P<0.01 | 0.74 | 1.57 | P<0.01 | 0.86 | 2.00 | P<0.01 |
| | NrF2 | 1.00 | 1.69 | P<0.01 | 1.30 | 2.34 | P<0.01 | 1.98 | 2.88 | P<0.01 |
| | KEAP-1 | 1.00 | 0.56 | P<0.01 | 2.62 | 2.47 | P>0.05 | 1.46 | 1.13 | P<0.05 |
| | GPR43 | 1.00 | 2.72 | P<0.01 | 0.40 | 0.46 | P>0.05 | 0.29 | 0.83 | P<0.05 |
| | GPR41 | 1.00 | 1.43 | P<0.01 | 1.22 | 2.19 | P<0.01 | 1.34 | 2.52 | P<0.01 |
| | GPR109a | 1.00 | 1.40 | P<0.01 | 1.16 | 1.72 | P<0.01 | 1.32 | 2.08 | P<0.01 |
| | MUC-2 | 1.00 | 1.32 | P<0.01 | 0.17 | 0.25 | P>0.05 | 0.18 | 0.31 | P<0.05 |
| | Notch-1 | 1.00 | 0.24 | P<0.05 | 0.07 | 0.01 | P<0.05 | 0.24 | 0.03 | P<0.05 |
| | Notch-2 | 1.00 | 0.57 | P<0.05 | 0.48 | 0.32 | P<0.05 | 0.40 | 0.15 | P<0.05 |
| **Duodenum** | PMCAIb | 1.00 | 2.70 | P<0.01 | 0.17 | 1.49 | P<0.01 | 0.59 | 0.75 | P<0.05 |
| | CaBP-D28K | 1.00 | 1.15 | P>0.05 | 2.52 | 3.07 | P<0.01 | 0.92 | 1.61 | P<0.01 |
| | NPt2a | 1.00 | 1.22 | P<0.01 | 0.15 | 0.74 | P<0.01 | 1.28 | 1.16 | P>0.05 |
| | NPt2b | 1.00 | 1.28 | P<0.01 | 0.90 | 1.69 | P<0.01 | 1.13 | 2.09 | P<0.01 |
| **Tibia** | IL-1B | 1.00 | 0.32 | P<0.01 | 1.40 | 0.53 | P<0.01 | 1.79 | 0.65 | P<0.01 |
| | TNF-α | 1.00 | 0.13 | P<0.01 | 0.95 | 0.23 | P<0.01 | 0.79 | 0.42 | P<0.01 |

| | | | | | | | | | |
|---|---|---|---|---|---|---|---|---|---|
| IL-18 | 1.00 | 0.58 | P<0.01 | 3.43 | 1.55 | P<0.01 | 1.50 | 1.12 | P<0.05 |
| IL-10 | 1.00 | 1.19 | P>0.05 | 0.46 | 1.59 | P<0.01 | 0.26 | 2.54 | P<0.01 |
| HIF-1α | 1.00 | 1.27 | P<0.01 | 0.54 | 0.85 | P<0.01 | 0.84 | 1.10 | P<0.05 |
| VEGFA | 1.00 | 1.24 | P<0.05 | 0.44 | 0.95 | P<0.01 | 1.09 | 1.23 | P<0.05 |
| ALP | 1.00 | 3.03 | P<0.01 | 1.54 | 4.97 | P<0.01 | 2.60 | 3.82 | P<0.05 |
| Wnt10b | 1.00 | 3.18 | P<0.01 | 1.88 | 3.79 | P<0.01 | 1.50 | 4.30 | P<0.01 |
| SMAD | 1.00 | 1.20 | P<0.01 | 0.22 | 1.53 | P<0.01 | 1.05 | 1.96 | P<0.01 |
| SOST | 1.00 | 2.09 | P<0.01 | 2.89 | 3.19 | P<0.01 | 0.94 | 1.24 | P<0.01 |
| OCN | 1.00 | 1.95 | P<0.01 | 0.34 | 1.93 | P<0.01 | 1.21 | 1.89 | P<0.01 |
| OPG | 1.00 | 4.26 | P<0.01 | 0.50 | 1.05 | P<0.01 | 1.24 | 1.42 | P>0.05 |
| TGF-B | 1.00 | 1.46 | P>0.05 | 0.75 | 2.00 | P<0.01 | 0.97 | 1.65 | P<0.01 |
| RUNX2 | 1.00 | 1.44 | P>0.05 | 1.21 | 2.59 | P<0.01 | 1.74 | 2.07 | P<0.05 |
| FGF23 | 1.00 | 1.41 | P<0.01 | 0.71 | 0.62 | P>0.05 | 1.34 | 2.07 | P<0.01 |
| PHEX | 1.00 | 1.47 | P<0.01 | 0.75 | 2.07 | P<0.01 | 0.89 | 3.16 | P<0.01 |
| DMPI | 1.00 | 1.48 | P<0.01 | 0.40 | 5.15 | P<0.01 | 1.24 | 3.15 | P<0.01 |
| MEPE | 1.00 | 4.74 | P<0.01 | 1.33 | 5.22 | P<0.01 | 1.51 | 3.89 | P<0.01 |
| NF-κB | 1.00 | 0.97 | P>0.05 | 0.70 | 0.57 | P<0.05 | 0.79 | 0.45 | P<0.01 |
| RANKL | 1.00 | 0.35 | P<0.01 | 1.25 | 0.76 | P<0.05 | 3.34 | 1.42 | P<0.05 |
| TRAF6 | 1.00 | 0.32 | P<0.01 | 1.35 | 1.03 | P<0.05 | 0.71 | 0.53 | P<0.05 |
| NFATC1 | 1.00 | 0.39 | P<0.01 | 1.06 | 0.48 | P<0.01 | 2.28 | 1.04 | P<0.01 |
| MyD88 | 1.00 | 0.32 | P<0.01 | 1.40 | 0.53 | P<0.01 | 1.74 | 0.65 | P<0.01 |
| HDAC | 1.00 | 0.81 | P<0.01 | 2.10 | 1.47 | P<0.01 | 1.78 | 1.22 | P<0.01 |

**Figure 1.** Effect of perennial ryegrass on growth performance in meat geese. Figure 1 (a-c) represented average daily feed intake (ADFI), average daily gain (ADG) and feed conversion ratio (FCR) respectively. Figure 1 (d-h) indicated the Tibia characteristics. Figure 1(i-r) showed enhanced concentration of calcium, phosphorus, ALP, OCN (Bone formation marker) and decreased content of TRAP, NFATC-1 and TRAF-6 (Bone resorption markers). Figure 1s showed TD (tibial dyschondroplasia) lesions in meat geese. [a,b]Mean values with different letters are significantly different by one-way analysis of variance followed by Independent *T*-test ($p < 0.05$).

**Figure 2(a-b).** Representative micro CT images and the quantification of trabecular and cortical microstructure of tibia bone in meat geese at different stages. Perennial ryegrass supplementation improved the tibia microstructure of trabecular bone (Figure 2a) and cortical bone (Figure 2b) in meat geese.

**Figure 2(c-e).** Figure 2c represented Goldner trichome indicating mineralized (Yellow portion) and osteoid portion (Black arrow), Muscle fiber area (brown arrow) and collagen area (red portion). Figure 2d showed TRAP staining indicating osteoclast (black arrows) and SafraninO stain representing proteoglycan content (black arrow) as shown in the figure 2e. The asterisks symbol indicates significant differences *P < 0.05, **P < 0.01.

**Figure 3.** Perennial ryegrass intake increased the antioxidant status by reducing the oxidative stress at day 15, 30 and 60 in meat geese. Figure 8 (a-f) represented GSH-PX and CAT levels in the tibia, serum and ceca in meat geese. Figure 3 (g-i) represented MDA levels in the tibia, serum and bone marrow. Figure 3 (j-o) represented triglycerides, total cholesterol, LDL (low density lipoprotein), HDL (high density lipoprotein), BUN (blood urea nitrogen) and glucose levels in meat geese. Figure 3 (p-u) represented Estrogen, Vitamin D3, Serotonin (5-HT), Parathyroid hormone (PTH), Calcitonin (CT) and Insulin like growth factors (IGF-1) levels. Figure 3

(v-z, aa) represented the acetate, propionate, butyrate, iso-butyric acid, iso-valeric acid and valeric acid production in meat geese. [a,b]Mean values with different letters are significantly different by one-way analysis of variance followed by Independent *T*-test ($p < 0.05$). The asterisks symbol indicates significant differences *P < 0.05, **P < 0.01.

**Figure 4 (a-i).** Figure 4(a-c) represented the relative abundance of gut microbiota at phylum level. Figure 4(d-f) represented the alpha diversity at day 15, 30 and 60. Figure 4(g-i) represented the Beta diversity at day 15, 30 and 60.

**Figure 4 (j-o).** Figure 4(j-l) showed Circos diagram representing the relative abundance of gut microbiota at genus level. Figure 4(m-o) represented linear discriminant analysis (LDA) effect size (LefSe) in CD and CDA groups at day 15, 30 and 60.

**Figure 5.** Figure 5(a-c) represented the correlation between gut microbiota and SCFA's production. Figure 5(d-f) showed the correlation between SCFA's, immunity and gut barrier function. Figure 5(g-i) represented the correlation between SCFA's, tibia microstructure and bone markers

**Figure 6.** Representative intestinal morphological images using H&E staining, AB PAS staining of ileum and ceca respectively and Immunofluorescence (IF) analysis showing protein expression of tight junction protein in the cecal tissues of meat geese. Figure 6-l (a-h) represented the villus height (VH), villus width (VW), villus crypt depth (VCD), villus surface area (VSA), villus height: crypt depth (VH/CD) in the ileum, mucosal and muscularis thickness and goblet cells (ceca). Figure 6-ll (i-k) represented ZO-1, Claudin-1 and serum DAO. Blue: nucleus (DAPI); Red: ZO-1; Cerulean blue: merge of blue and red indicating nuclear localization of ZO-1, scale

bar = 20 µm. [a,b]Mean values with different letters are significantly different by one-way analysis of variance followed by Independent *T*-test ($p < 0.05$). The asterisks symbol indicates significant differences *P < 0.05, **P < 0.01.

**Figure 7.** Perennial ryegrass improved the immunity by reducing the inflammatory response in meat geese at day 15, 30 and 60. Figure 7 (a-r) represented IL-1B, IL-18, TNF- α, IL-10, LPS and ROS in the tibia, serum and ceca. Figure 7(s) represented western blot of Wnt-10b, Runx2, OCN, SMAD, ALP and OPG with GAPDH as reference. Figure 7(t) represented western blot of RANKL, NF-κB, NFATC-1 and HDAC. Figure 7(u) showed western blot of CaBP-28K, PMCA1b, NPt2a, PHEX, FGF-23. Figure 15(v) represented western blot of VEGFA and HIF-1. The asterisks symbol indicates significant differences *P < 0.05, **P < 0.01.

**Figure 8.** Figure 8(a) represented immunofluorescence (IF) analysis using Rabbit Anti-NF-κB (CY2339) (1:500/1:200) showing nuclear translocation of NF-κB in the tibia of meat geese. Blue: nucleus (DAPI); Red: NF-κB staining; Merge; combination of blue and red indicating nuclear translocation of NF-κB, scale bar = 200um. Figure 8(b) showed Immunofluorescence (IF) analysis using Rabbit Anti-Wnt10b (67201-1-IG) (1:500/1:200) showing nuclear translocation of Wnt10b in the tibia of meat geese. Blue: nucleus (DAPI); Red: WNT10b staining; Merge; combination of blue and red indicating nuclear translocation of Wnt10b, scale bar = 200um.

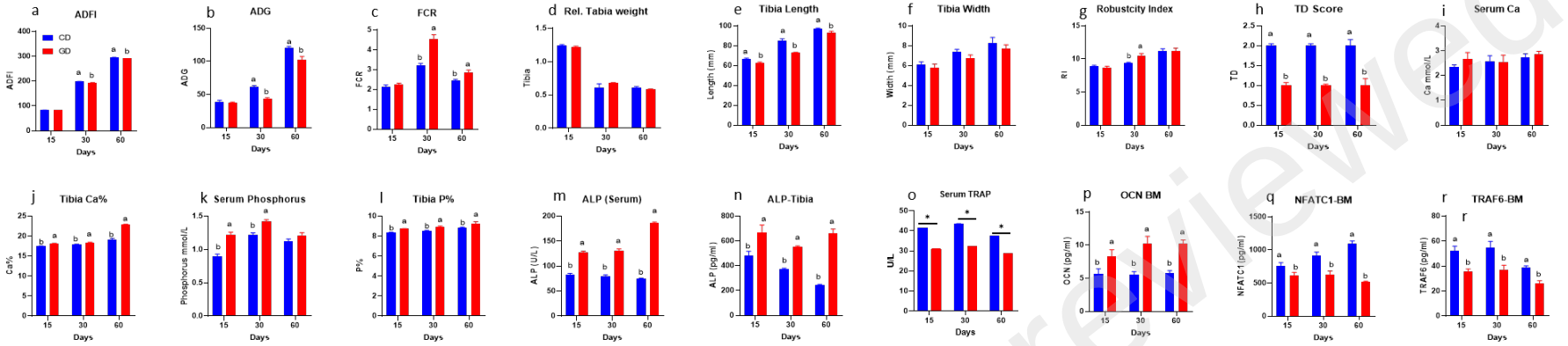


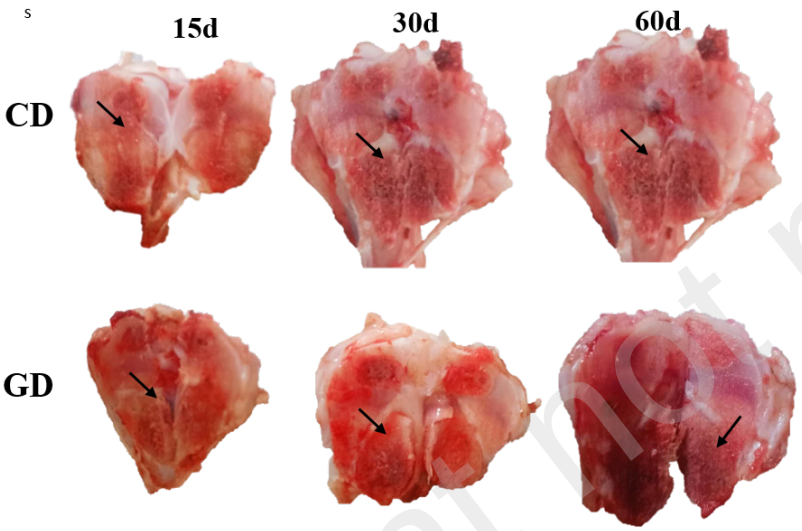

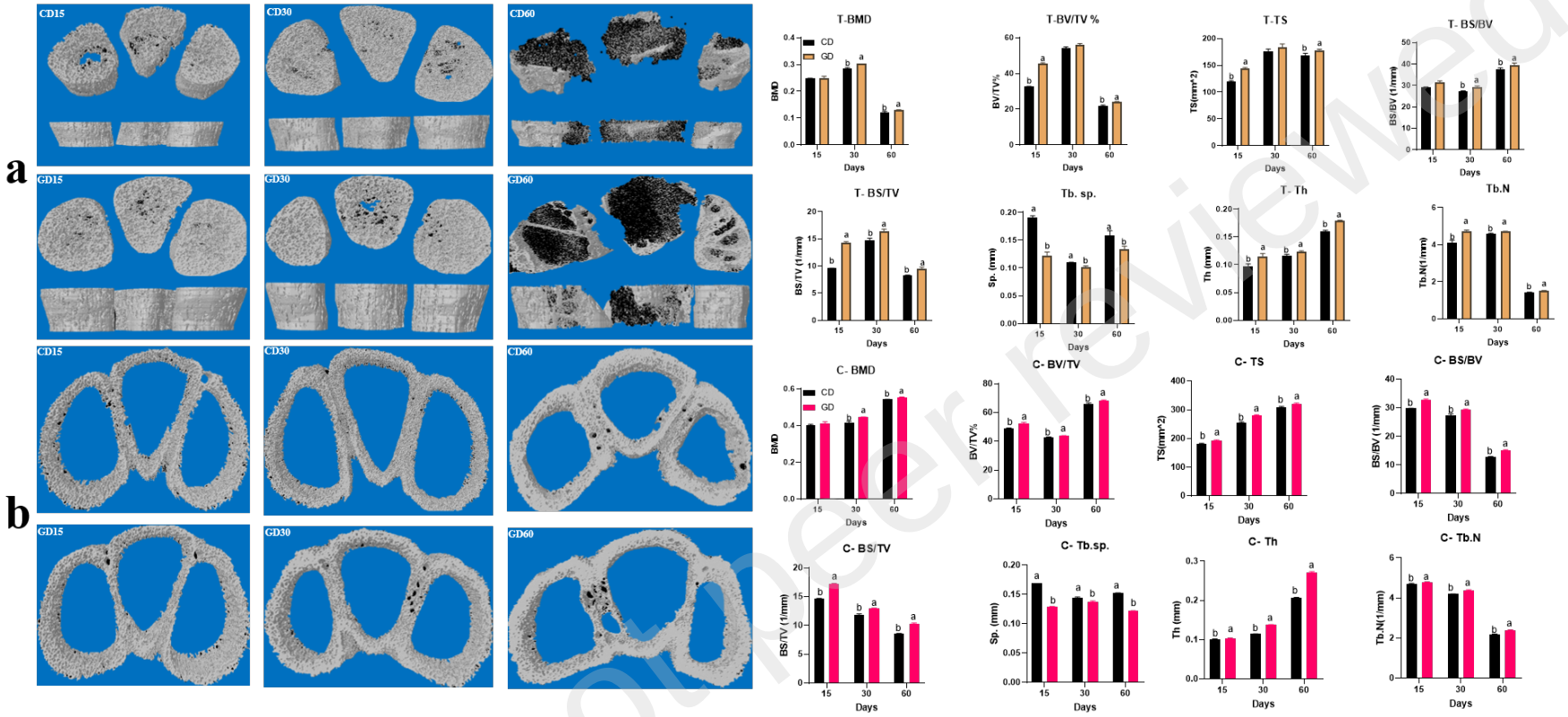

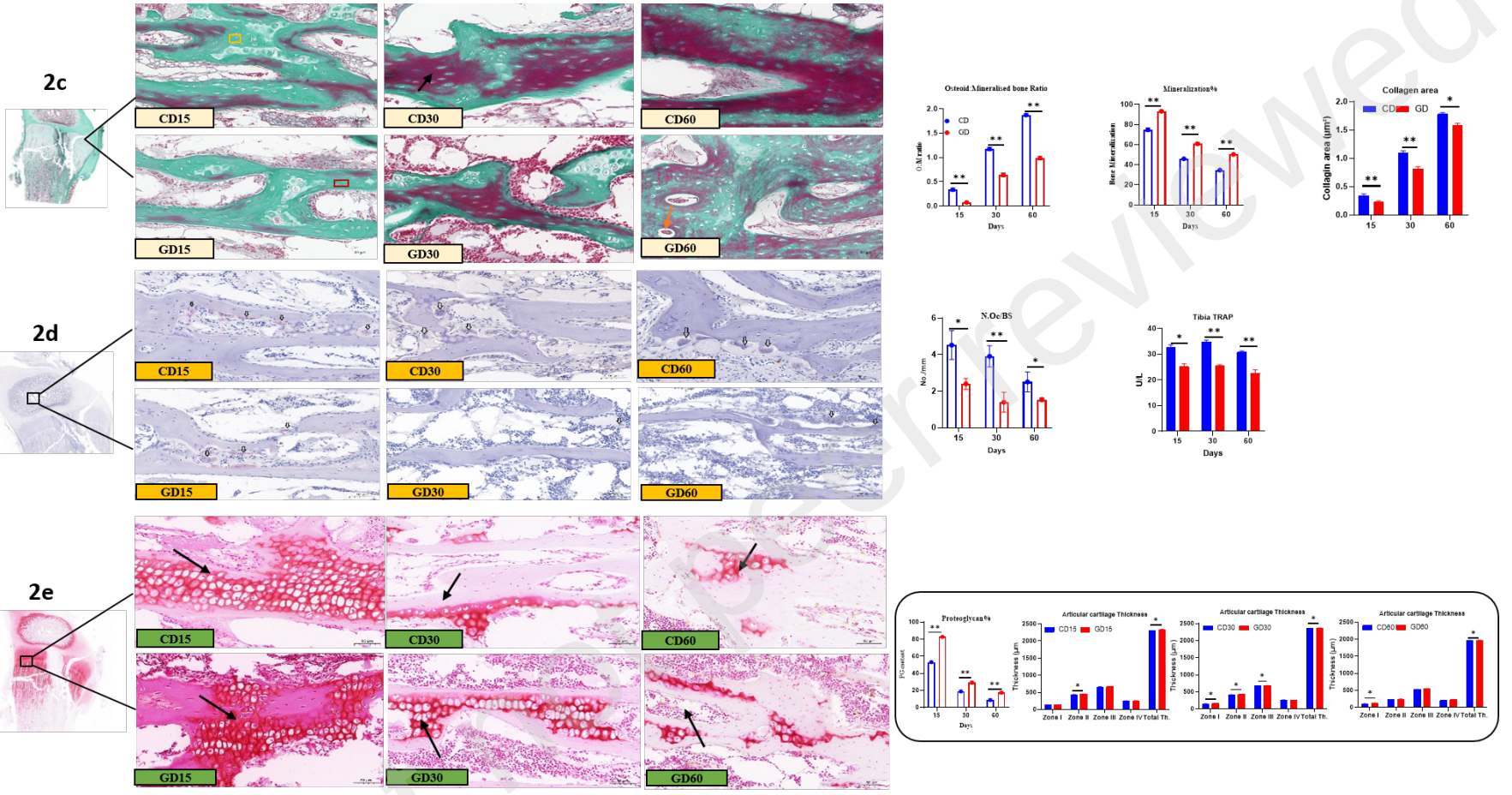

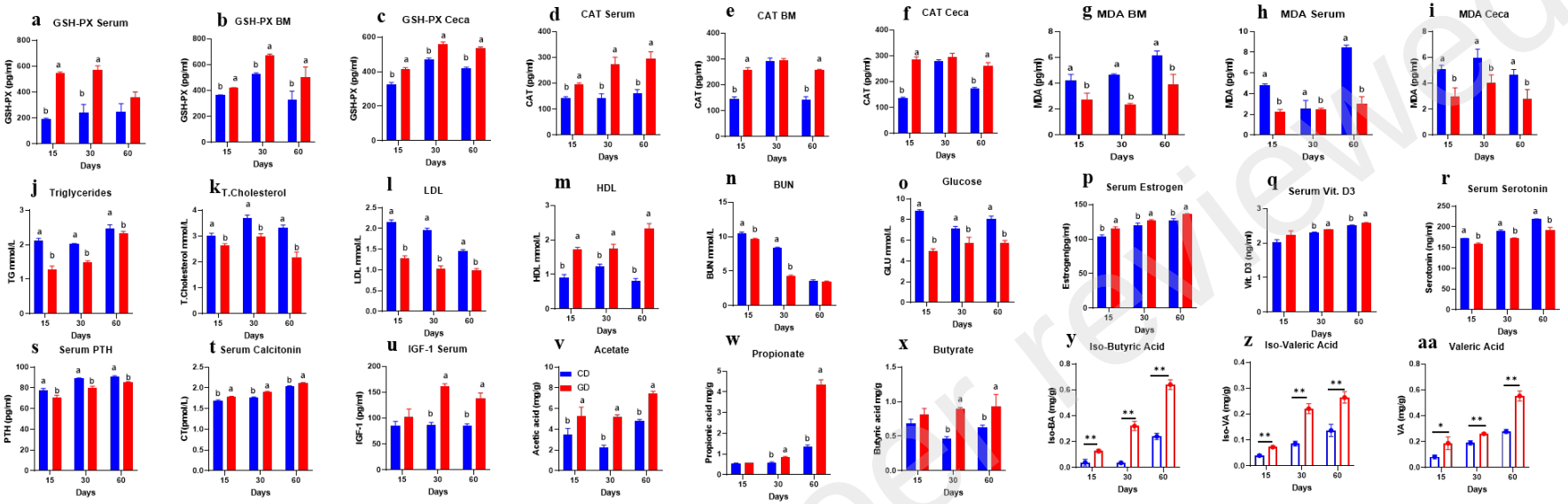

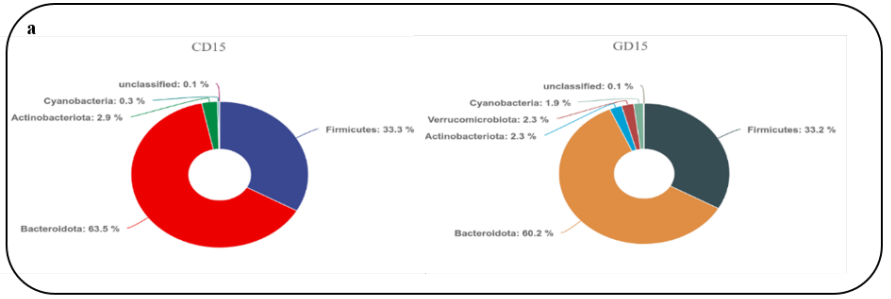


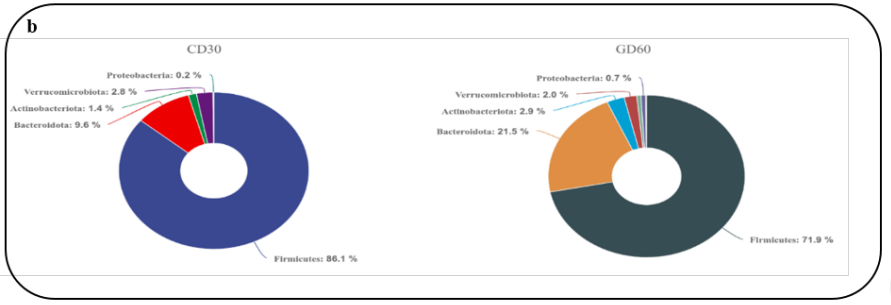


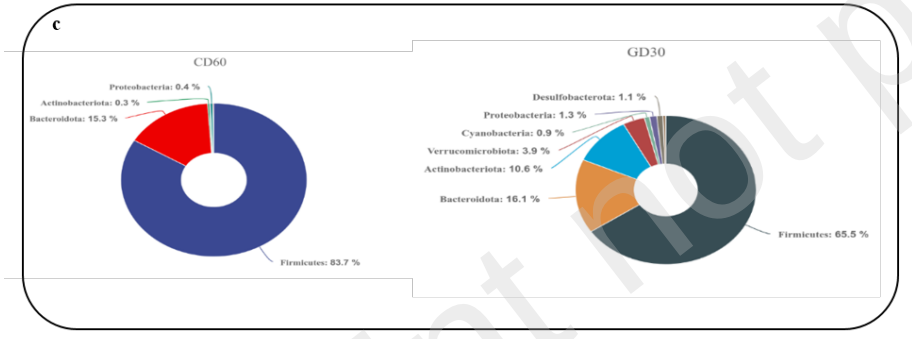


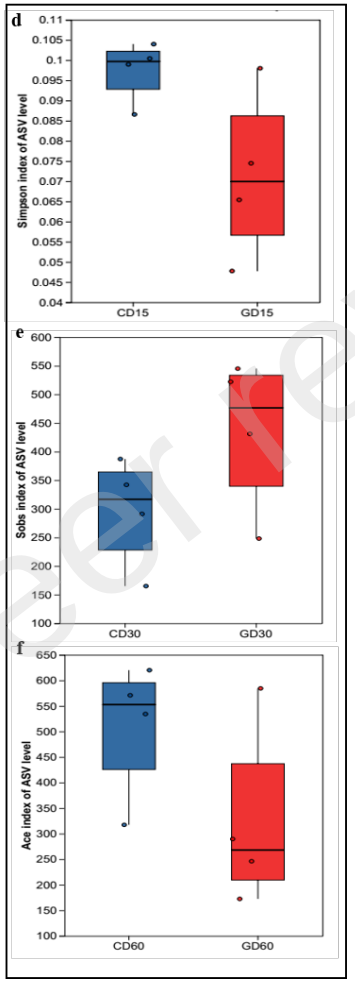


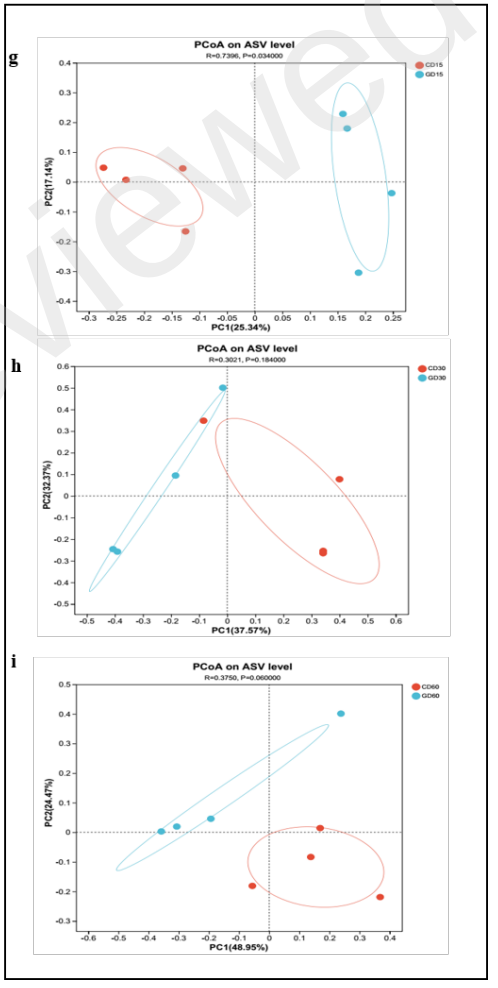

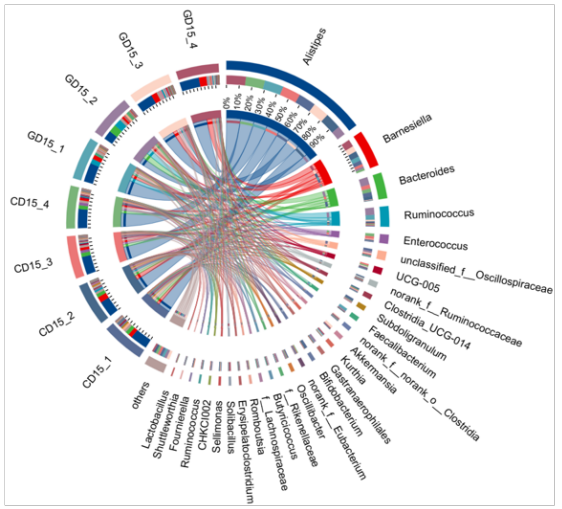


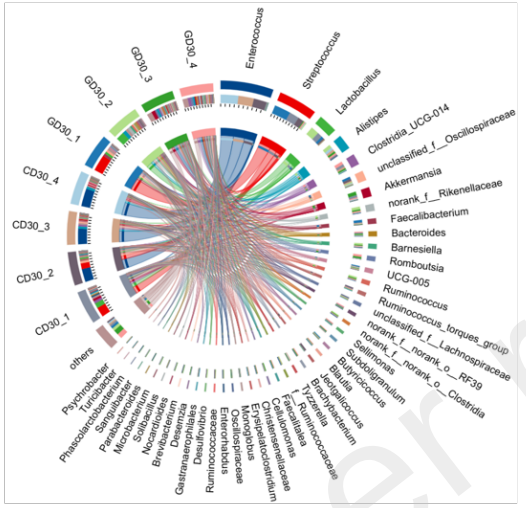


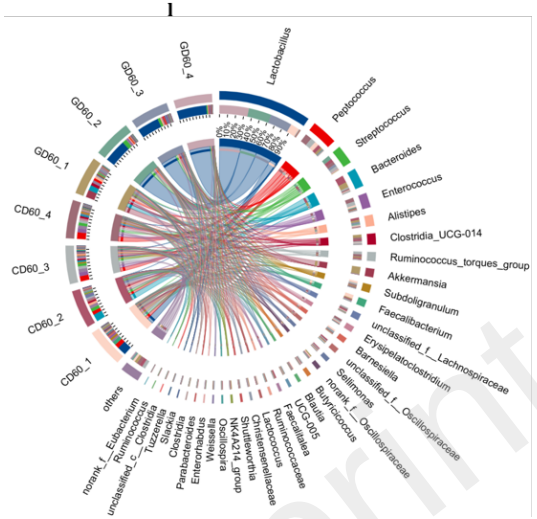


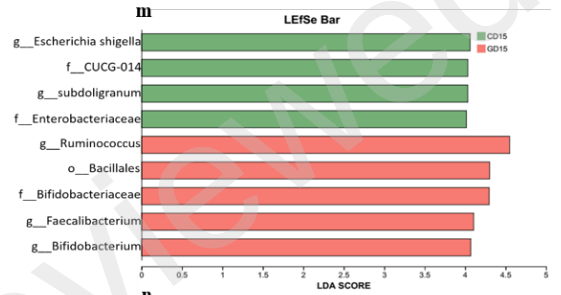


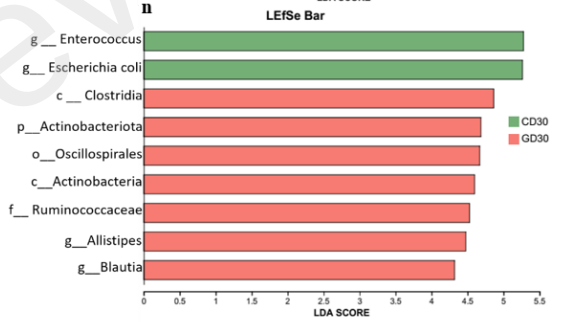


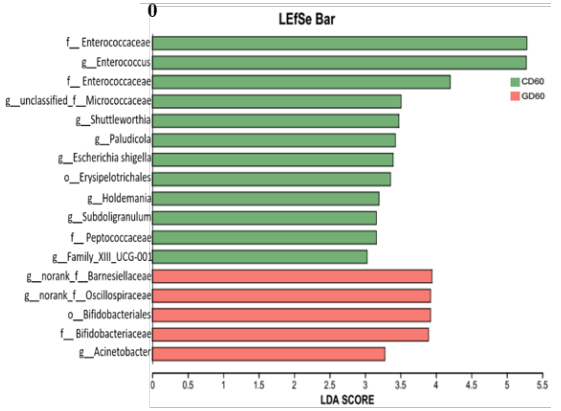

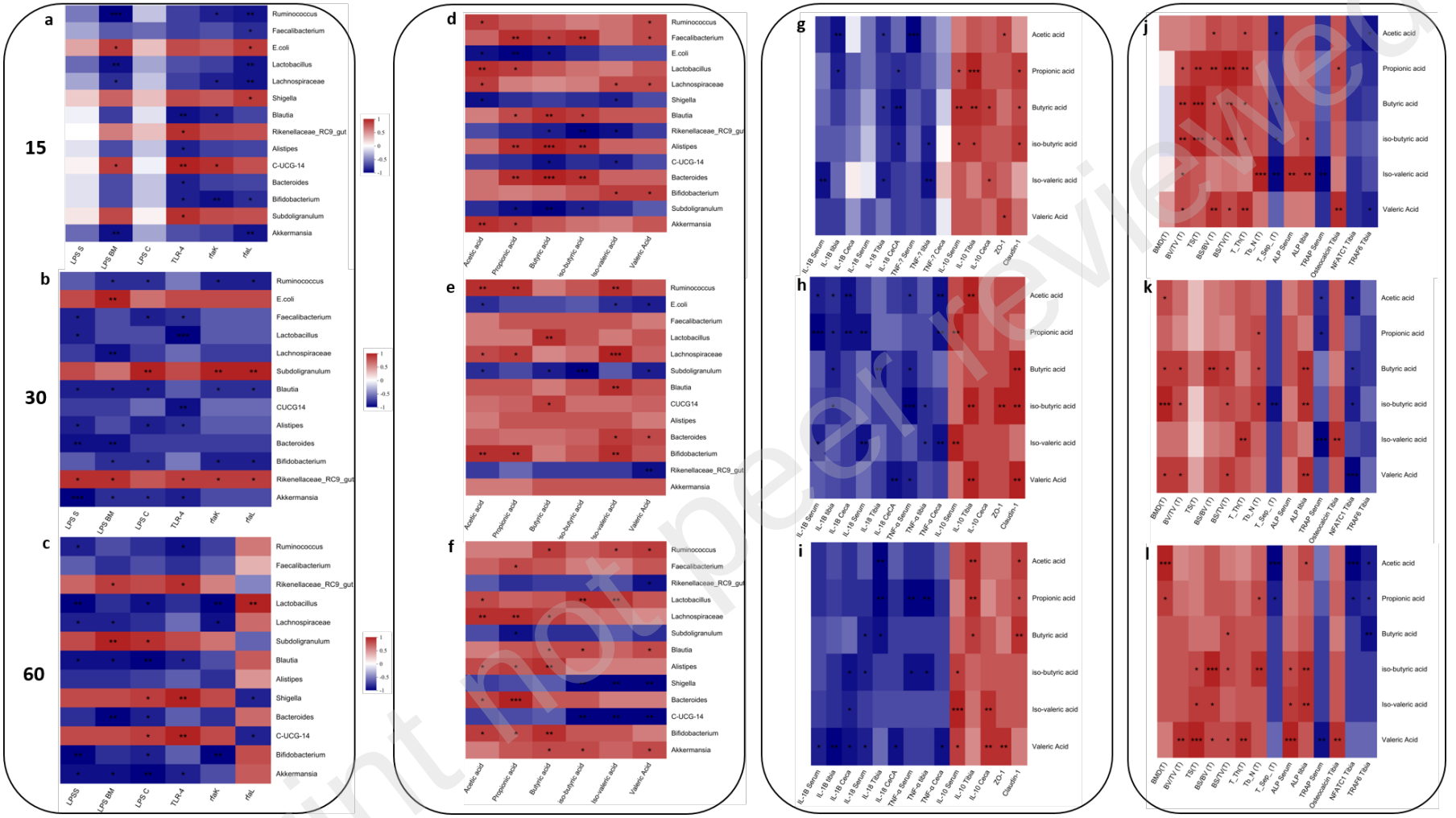

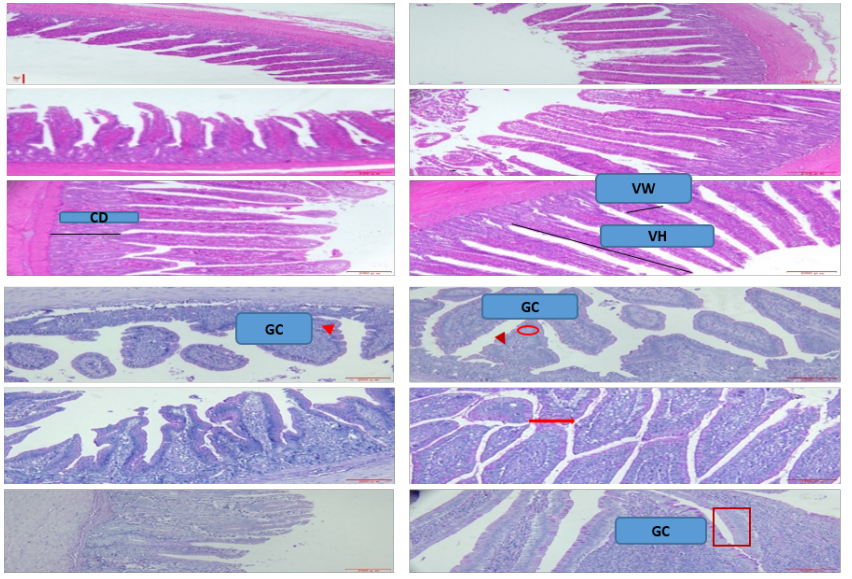


6-I

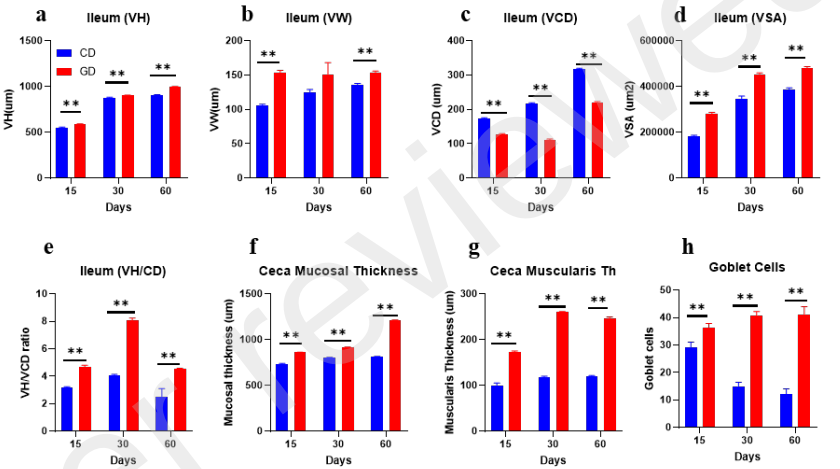


6-II

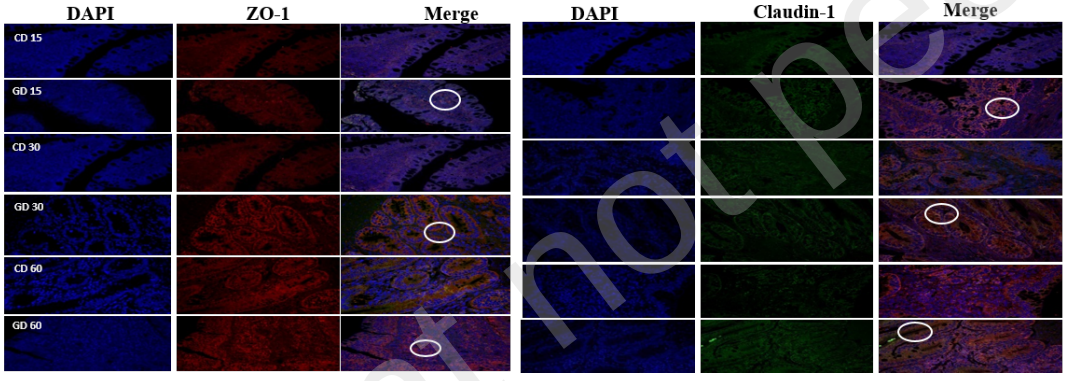


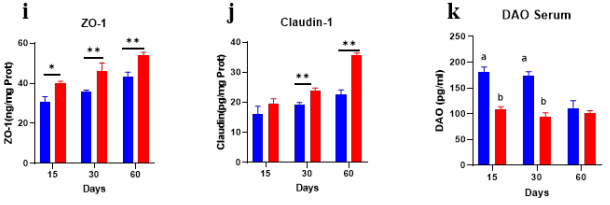

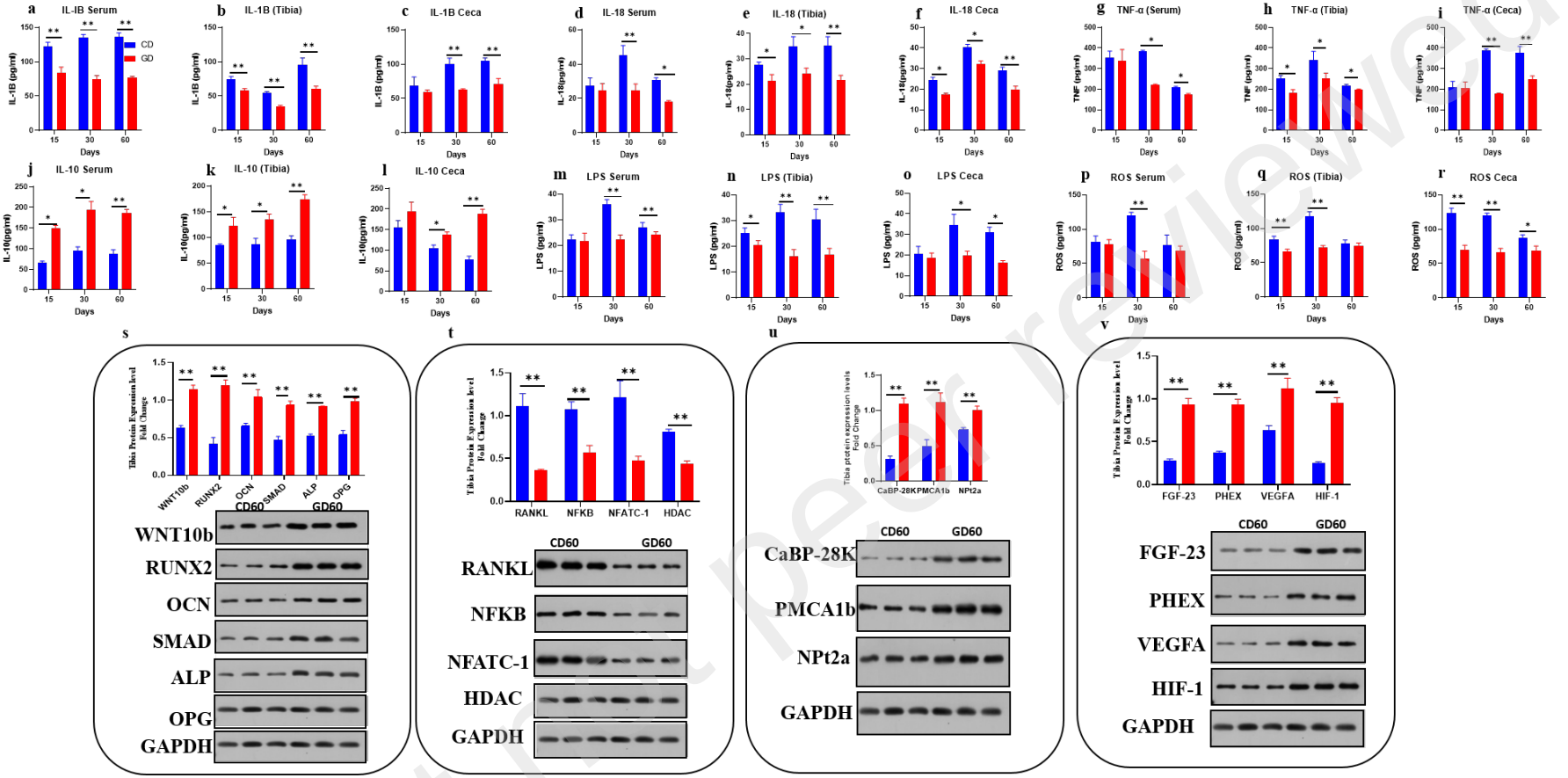

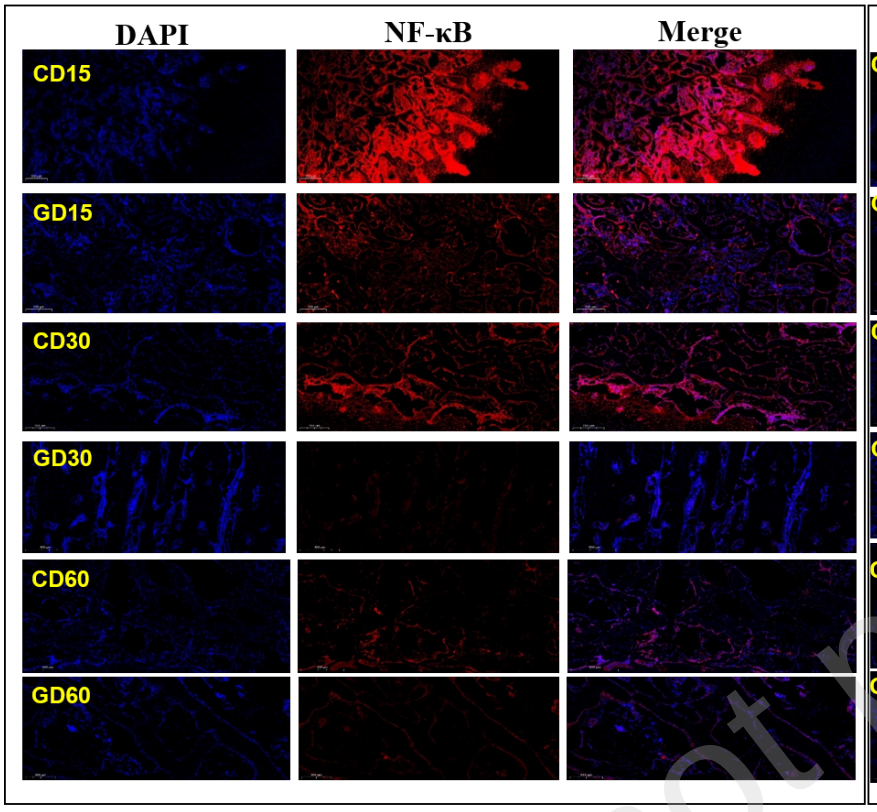


(a)

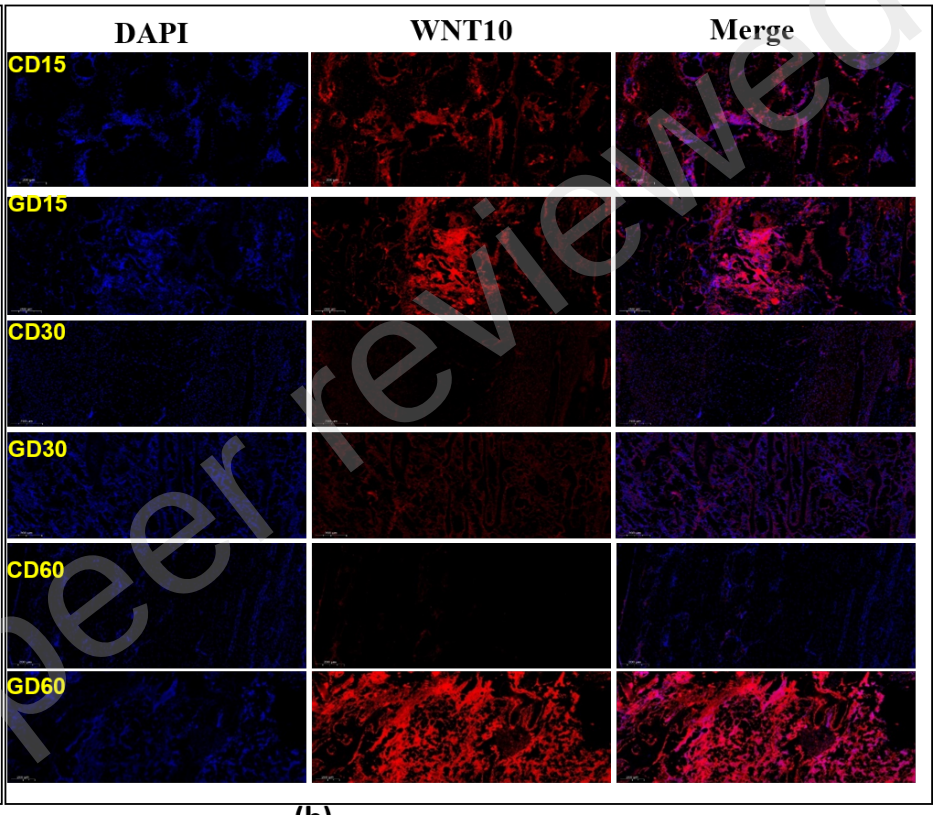


(b)